Dynamic Causal Modelling for fMRI: advanced topics

J. Daunizeau

Brain and Spine Institute, Paris, France

Wellcome Trust Centre for Neuroimaging, London, UK

Overview

1. Embedding computational models in DCM
2. Integrating tractography with DCM
3. Stochastic DCM
4. Optimizing experimental design
5. Searching through large model spaces
6. Some diagnostic on inversion results
7. Experimental validation and perspectives

Overview

1. Embedding computational models in DCM
2. Integrating tractography with DCM
3. Stochastic DCM
4. Optimizing experimental design
5. Searching through large model spaces
6. Some diagnostic on inversion results
7. Experimental validation and perspectives

Embedding computational models in DCM

example: audiovisual associative learning (I)

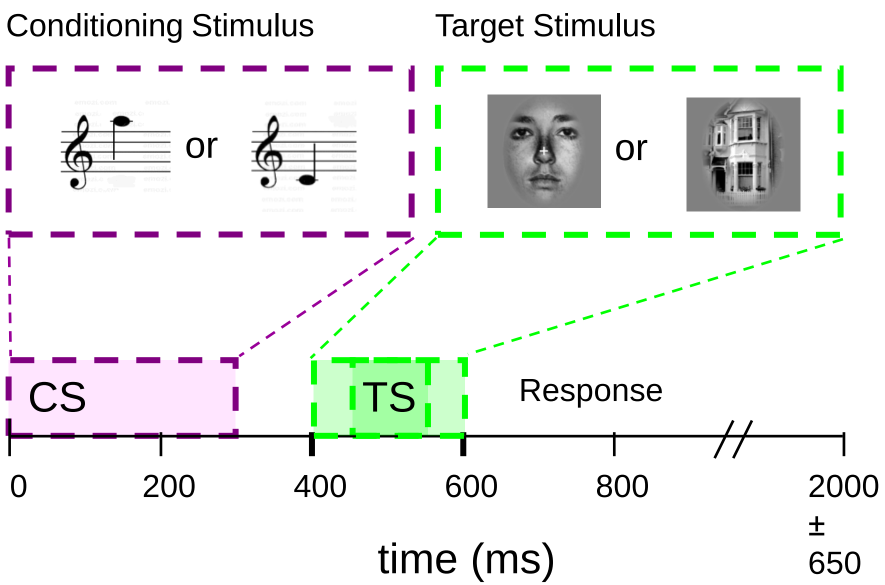

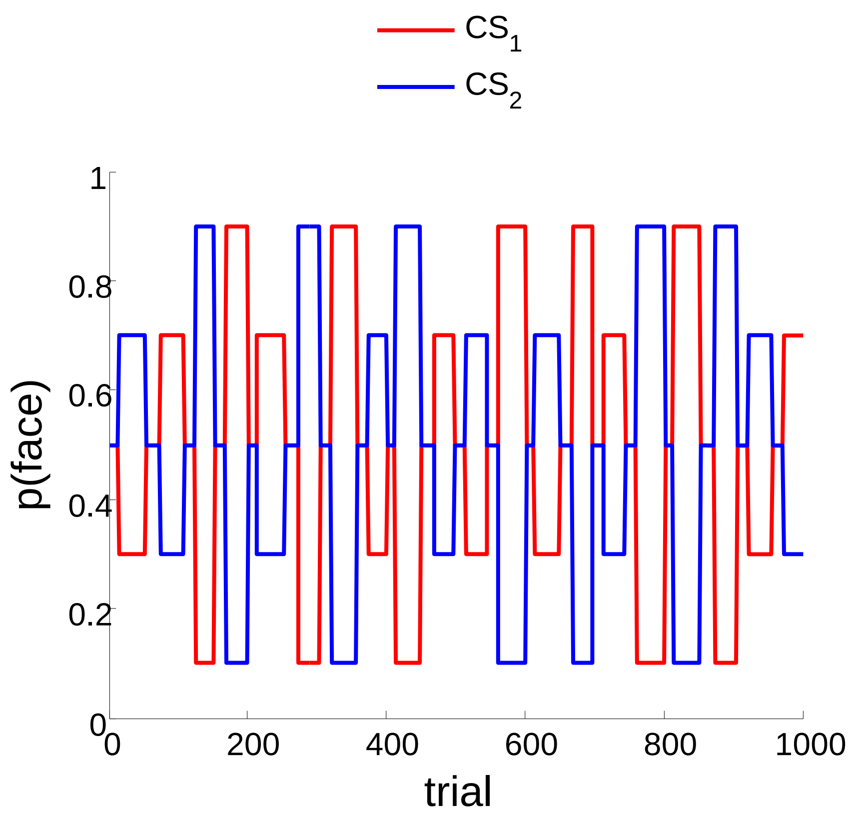

Den Ouden et al., 2010

Embedding computational models in DCM

example : audiovisual associative learning (II)

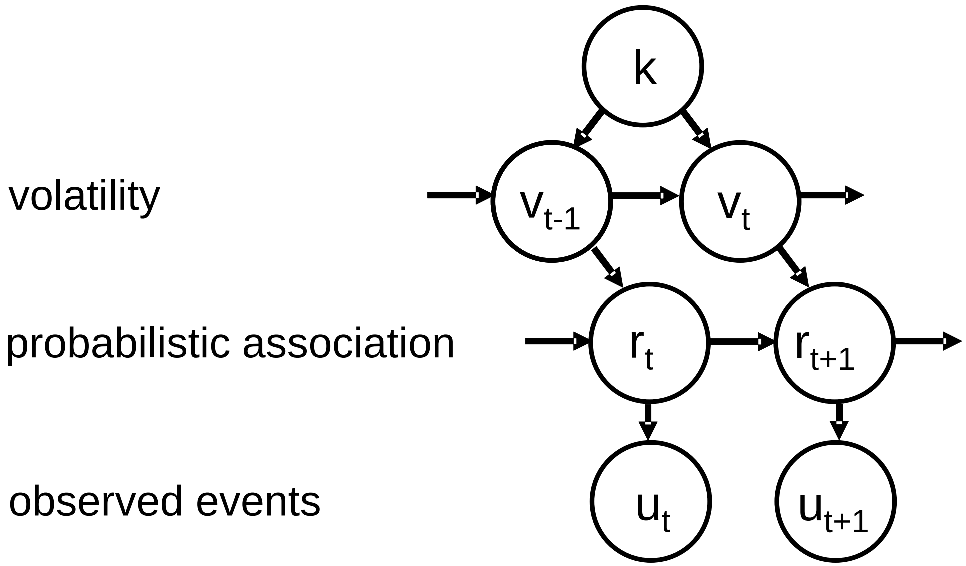

$$p(k) \propto 1$$

$$p(v_{t+1} \mid v_t, k) \sim N(v_t, \exp(k))$$

$$p(r_{t+1} \mid r_t, v_t) \sim Dir(r_t, \exp(v_t))$$

prediction: $p\left(r_t, v_t, K \middle| u_{1:t-1}\right) = \iint p\left(r_t \middle| r_{t-1}, v_{t-1}\right) p\left(v_t \middle| v_{t-1}, K\right) p\left(r_{t-1}, v_{t-1}, K \middle| u_{1:t-1}\right) dr_{t-1} dv_{t-1}$

update: $p\left(r_t, v_t, K \middle| u_{1:t}\right) = \dfrac{p\left(r_t, v_t, K \middle| u_{1:t-1}\right) p\left(u_t \middle| r_t\right)}{\iiint p\left(r_t, v_t, K \middle| u_{1:t-1}\right) p\left(u_t \middle| r_t\right) dr_t dv_t dK}$

Behrens et al., 2007

Embedding computational models in DCM

example : audiovisual associative learning (III)

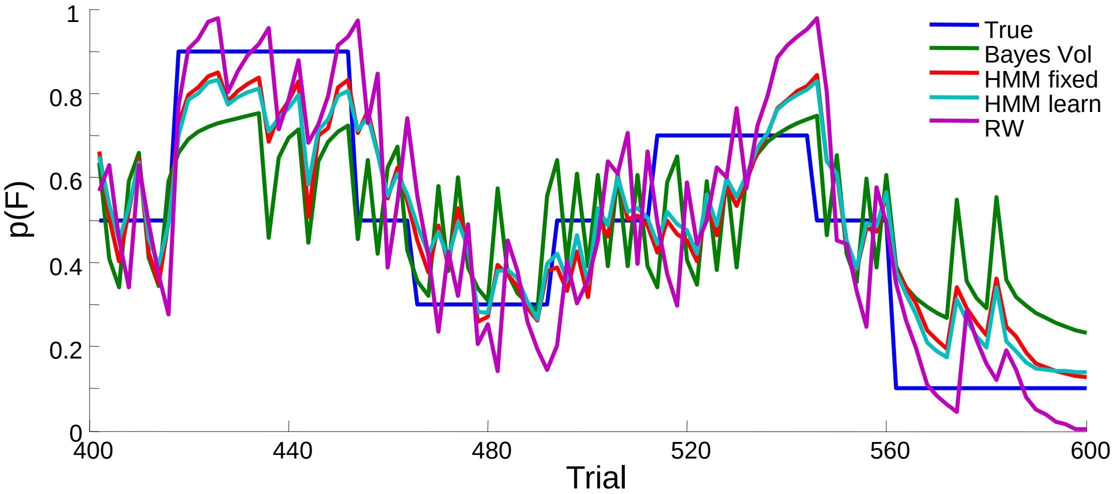

Alternative learning models:

- Rescorla-Wagner
- HMM (2 variants)
- True probabilities

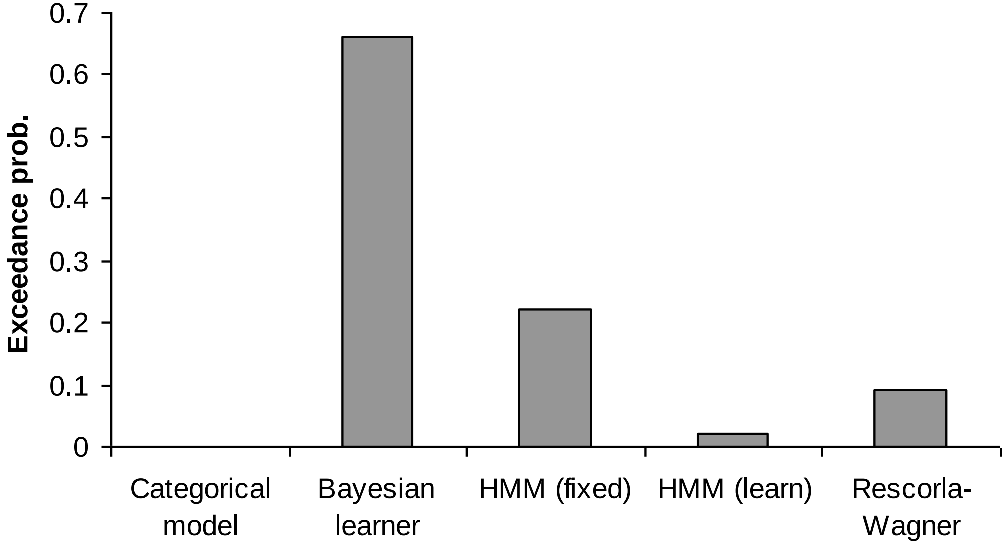

BMS:

hierarchical Bayesian learner performs best

Den Ouden et al., 2010

Embedding computational models in DCM

example : audiovisual associative learning (IV)

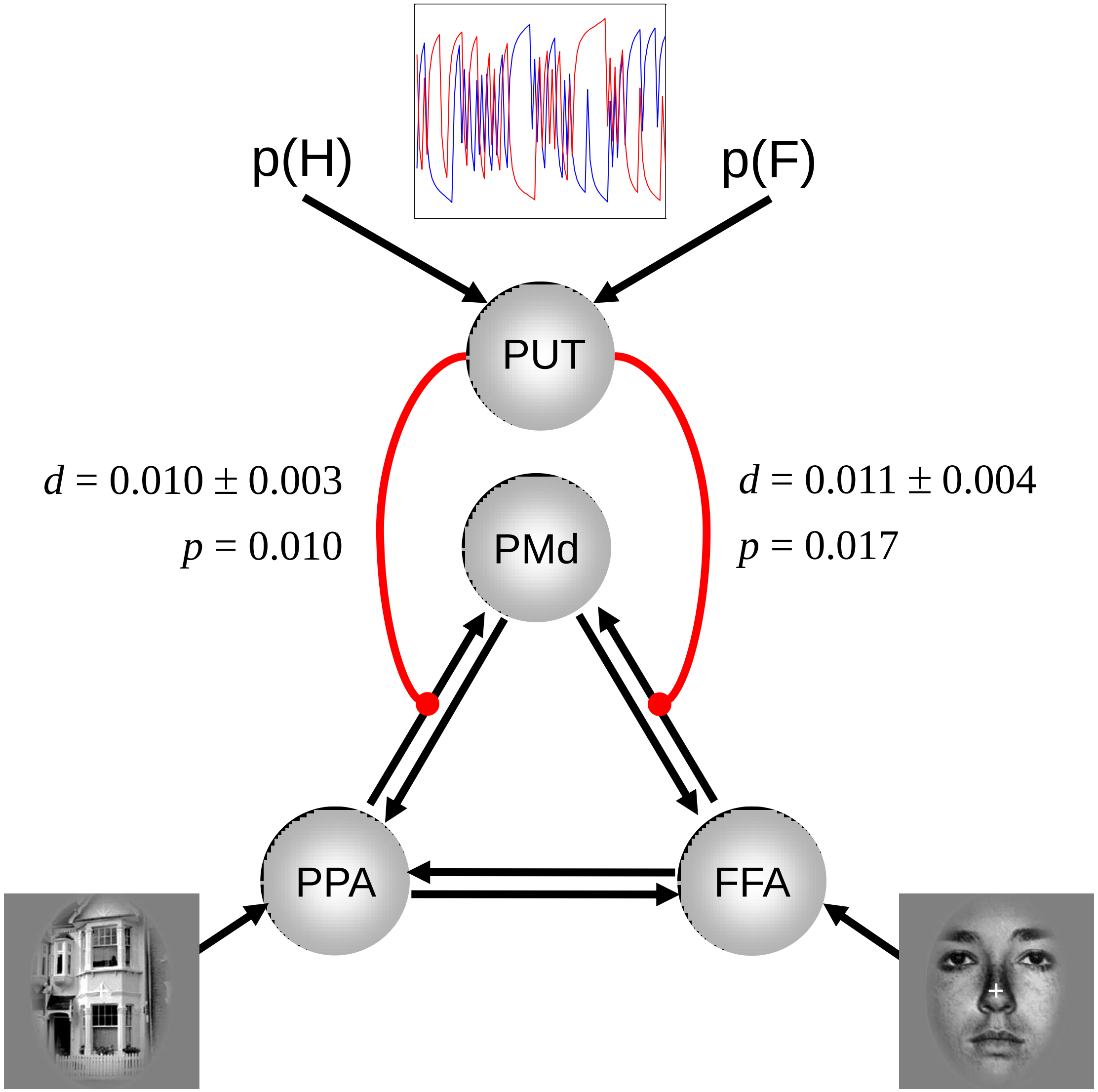

- Modulation of visuo-motor connections by striatal PE activity
- Influence of visual areas on premotor cortex:
  - stronger for surprising stimuli
  - weaker for expected stimuli

Den Ouden et al., 2010

Overview

1. Embedding computational models in DCM
2. Integrating tractography with DCM
3. Stochastic DCM
4. Optimizing experimental design
5. Searching through large model spaces
6. Some diagnostic on inversion results
7. Experimental validation and perspectives

Integrating tractography and DCM
the nature of DWI information

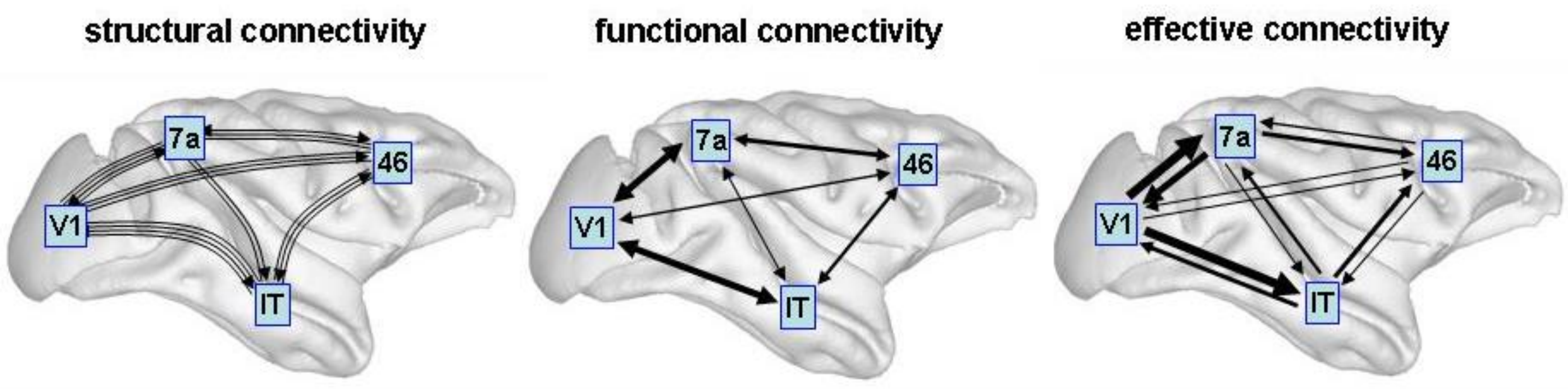

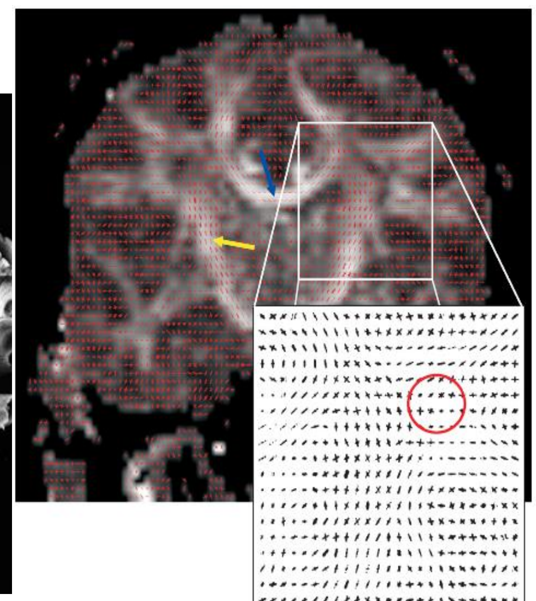

Parker et al., 2005

Integrating tractography and DCM
probabilistic tractography

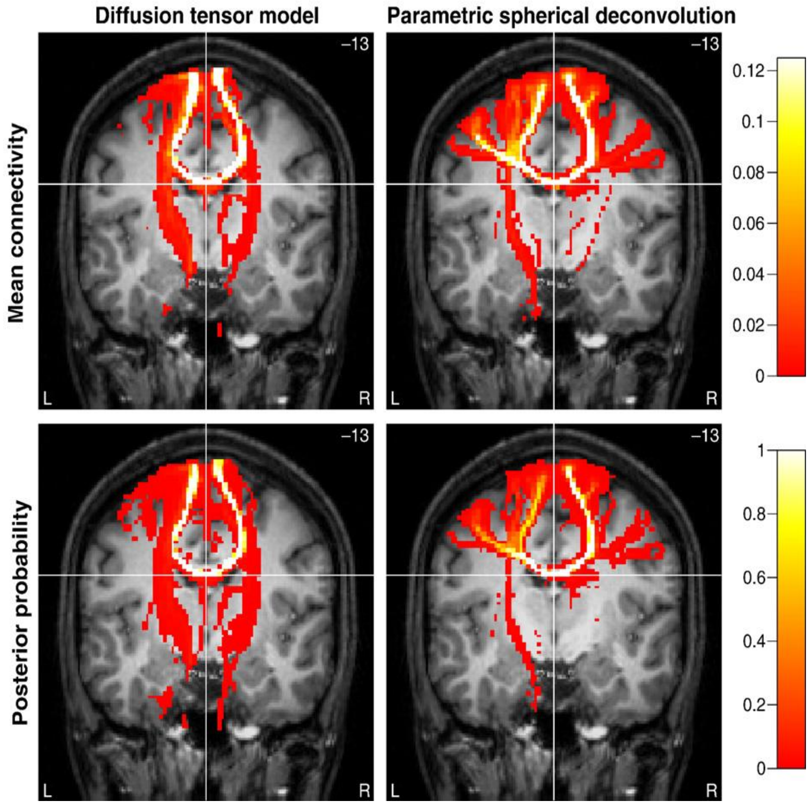

- computes local fibre orientation density by deconvolution of the diffusion-weighted signal
- estimates the spatial probability distribution of connectivity from given seed regions
- anatomical connectivity = proportion of fibre pathways originating in a specific source region that intersect a target region
- Asymmetry in metric accounted for by taking average of seed and target regions when interchanged

Kaden et al., 2007

Integrating tractography and DCM

integrating tractographic prior information into DCM

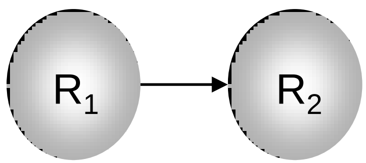

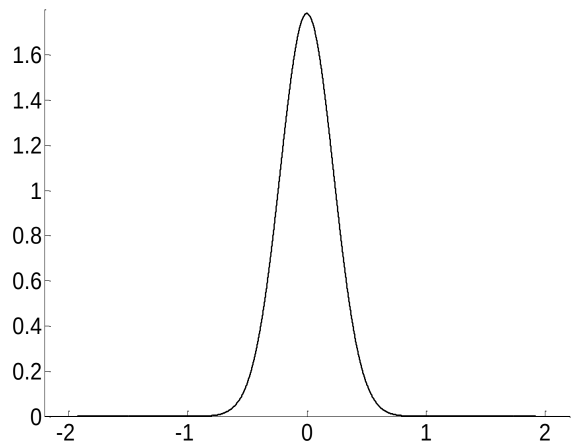

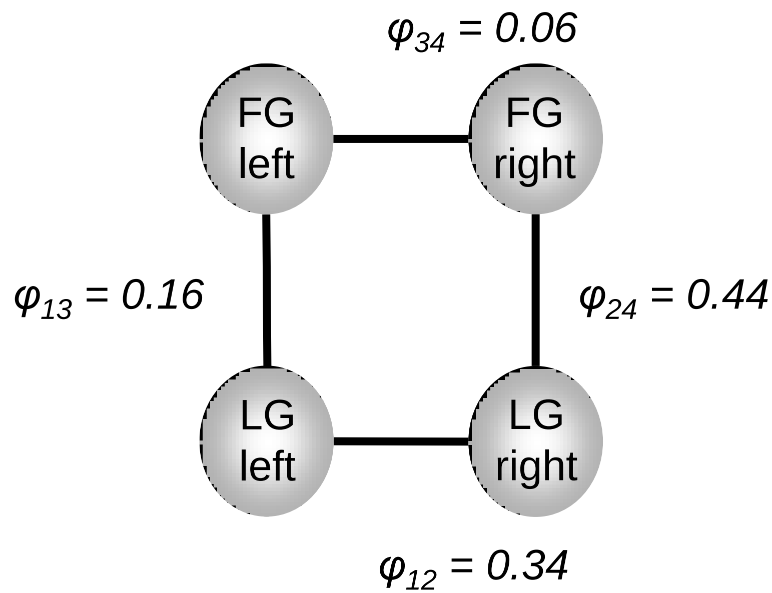

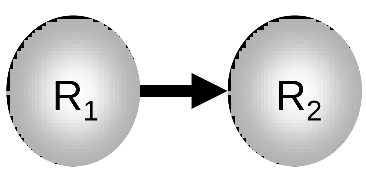

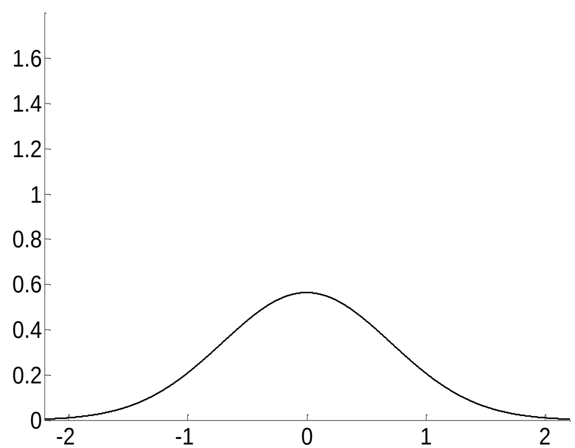

$$\Sigma_{ij} = \frac{\Sigma_0}{1 + \Sigma_0 \exp(\alpha - \beta \varphi_{ij})}$$

Stephan et al., 2009

Integrating tractography and DCM

searching through the space of structure-function mappings

- 64 different mappings by systematic search across hyper-parameters α and β

- yields anatomically informed (intuitive and counterintuitive) and uninformed priors

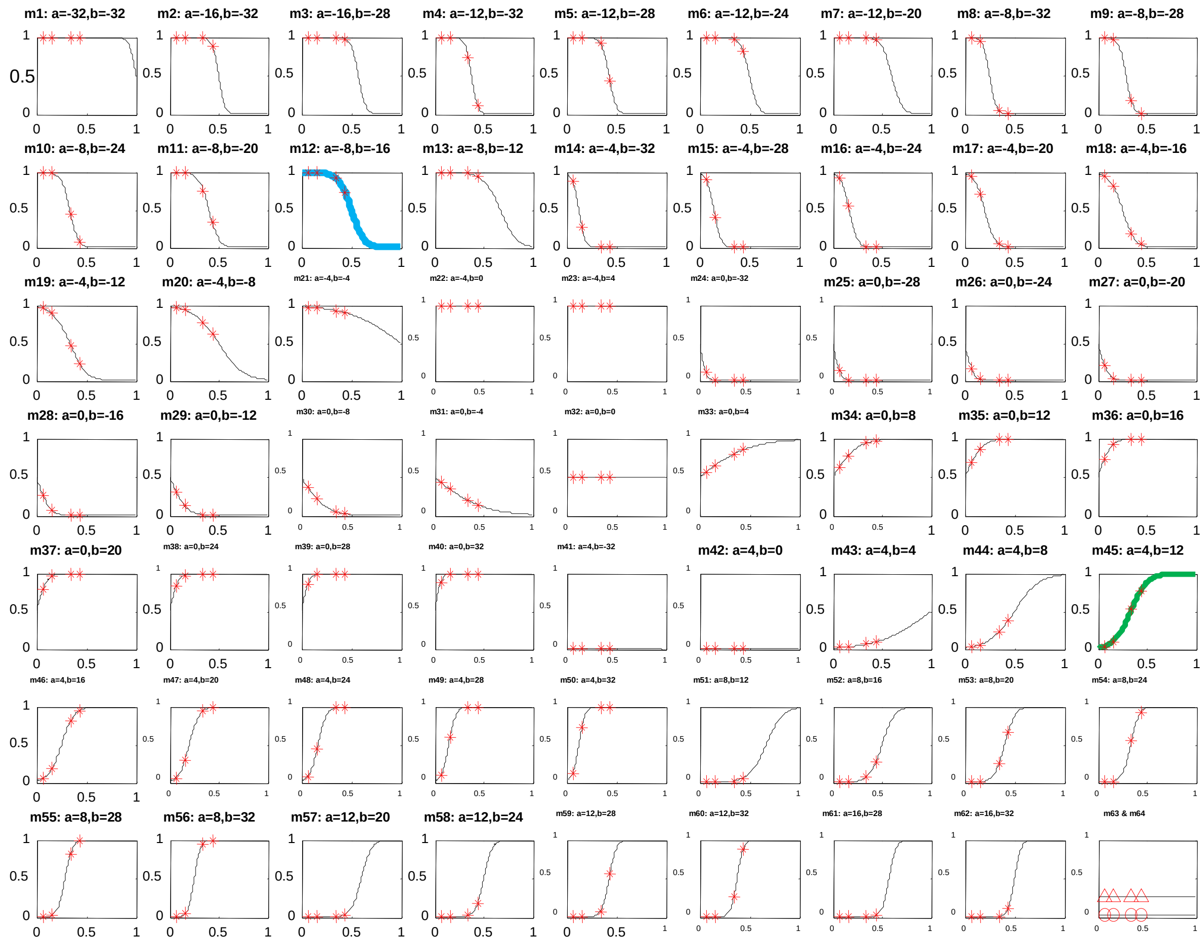

Stephan et al., 2009

Integrating tractography and DCM

structure-function mappings: group BMC results (I)

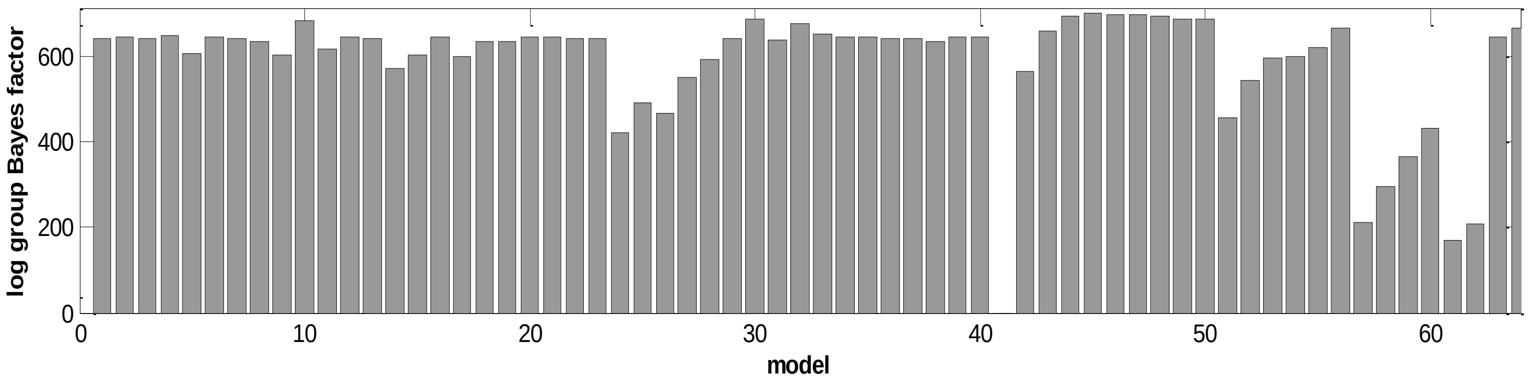

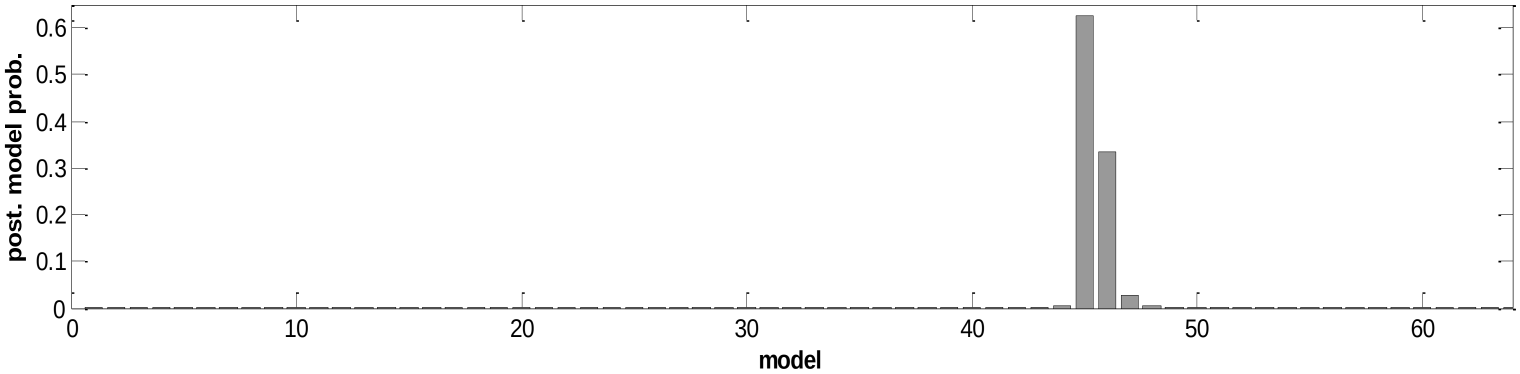

Stephan et al., 2009

Integrating tractography and DCM

structure-function mappings: group BMC results (II)

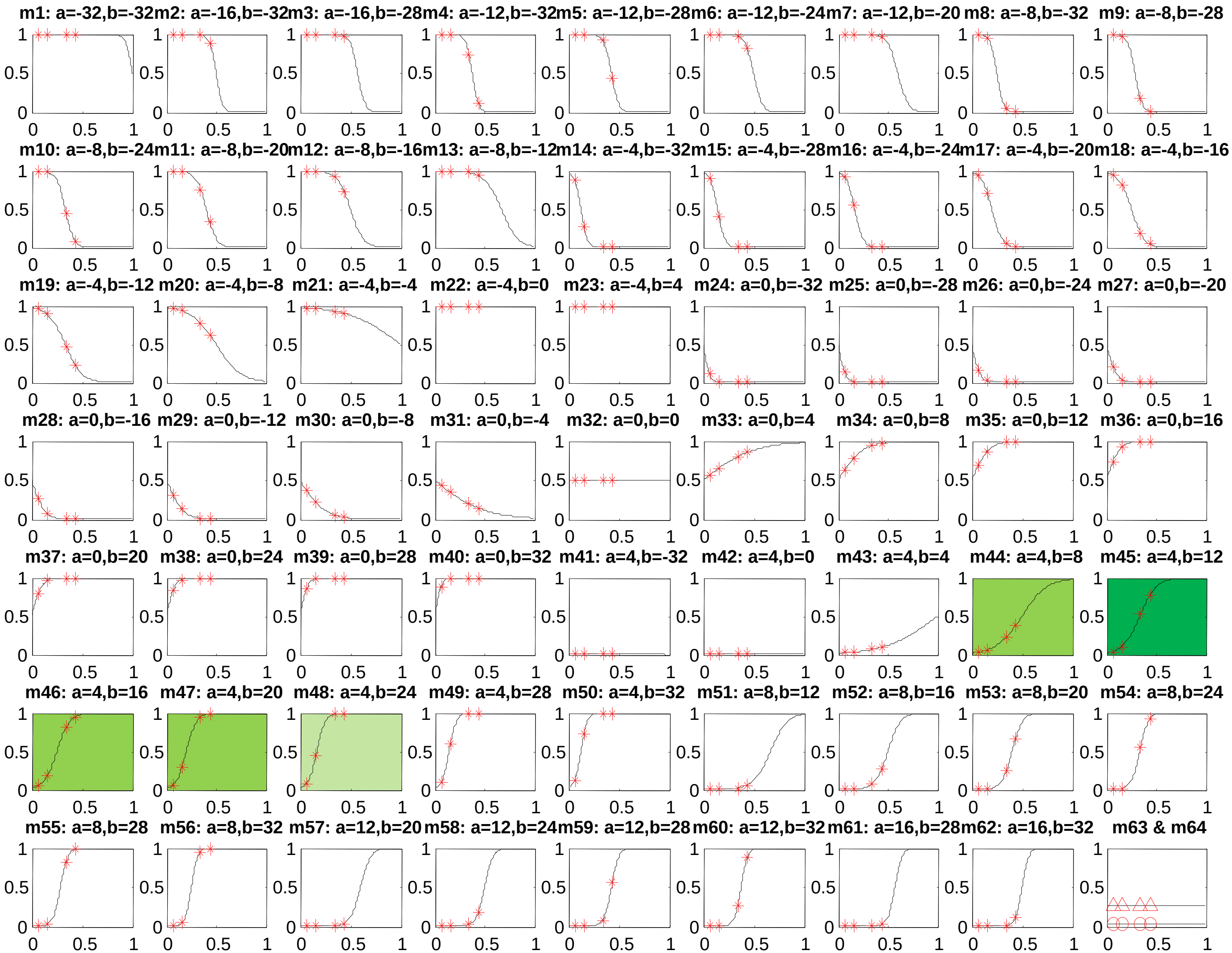

Stephan et al., 2009

Overview

1. Embedding computational models in DCM
2. Integrating tractography with DCM
3. Stochastic DCM
4. Optimizing experimental design
5. Searching through large model spaces
6. Some diagnostic on inversion results
7. Experimental validation and perspectives

Stochastic DCM for fMRI

the effect of state noise on network dynamics

$$\dot{x} = f\left(x, \theta, u\right) + \eta$$

neural noise:

- model imperfections
- ongoing fluctuations

2-regions DCM structure

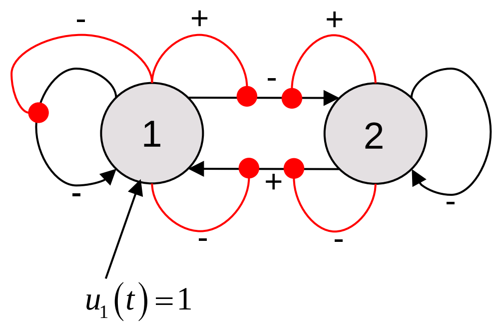

moving frame of reference

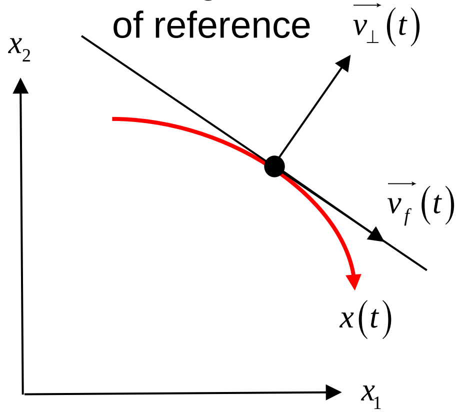

state-space landscape of the normal rate of convergence $\lambda_{\perp\perp}(x)$

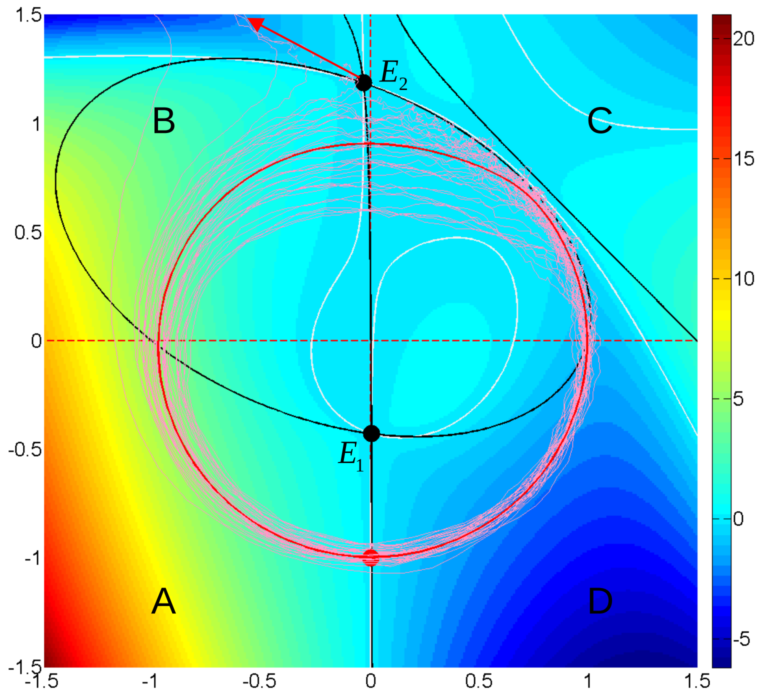

Daunizeau et al., 2012

Stochastic DCM for fMRI

mediated influence: canonical model comparison

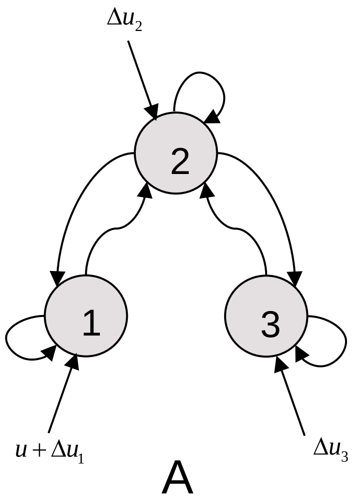

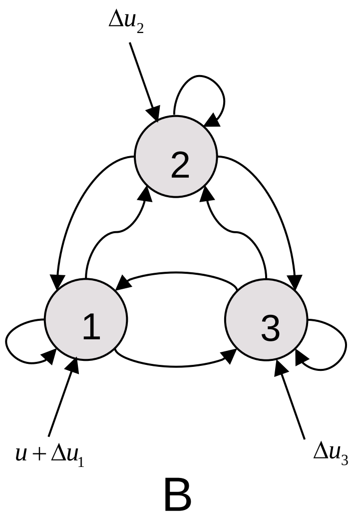

Model comparison: evidence against the full model

$$LBF_{AB} = \log \frac{p(y|A,m)}{p(y|B,m)}$$

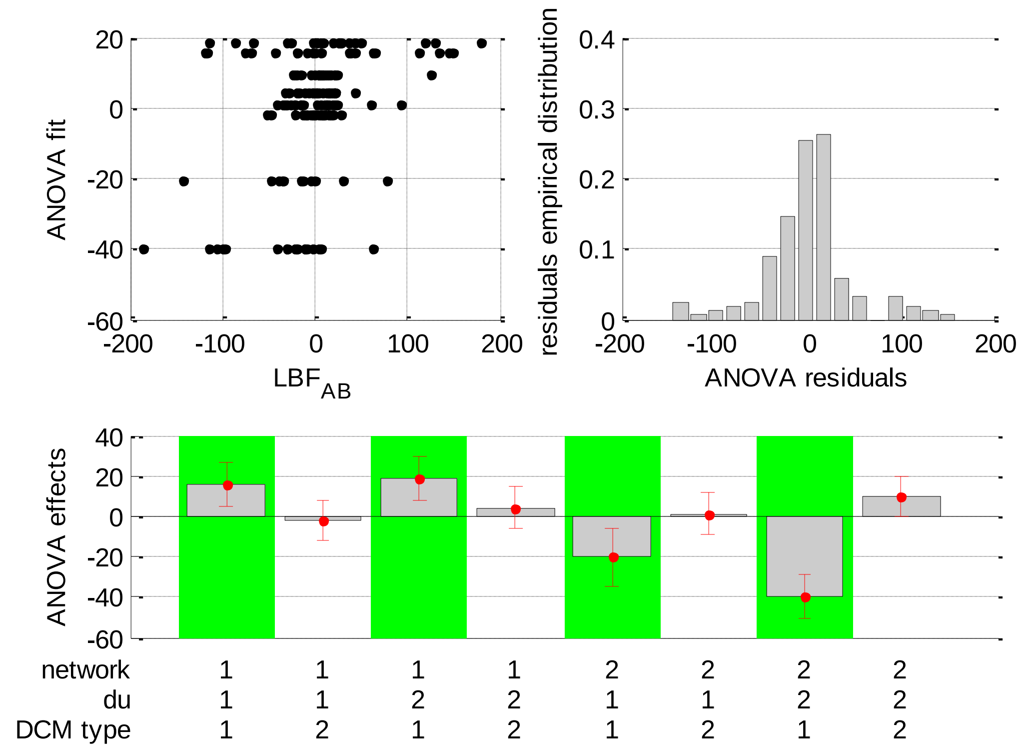

Daunizeau et al., 2012

Stochastic DCM for fMRI

example: epileptogenic network

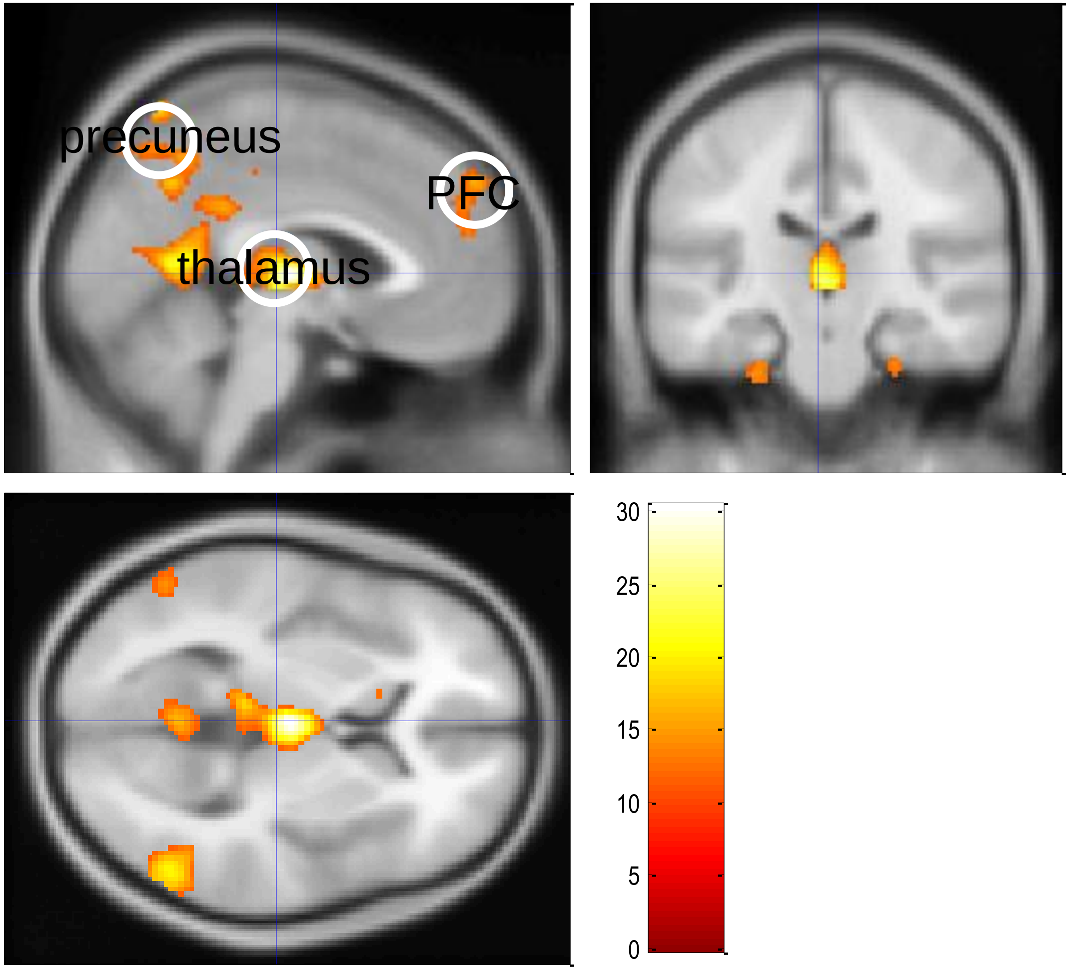

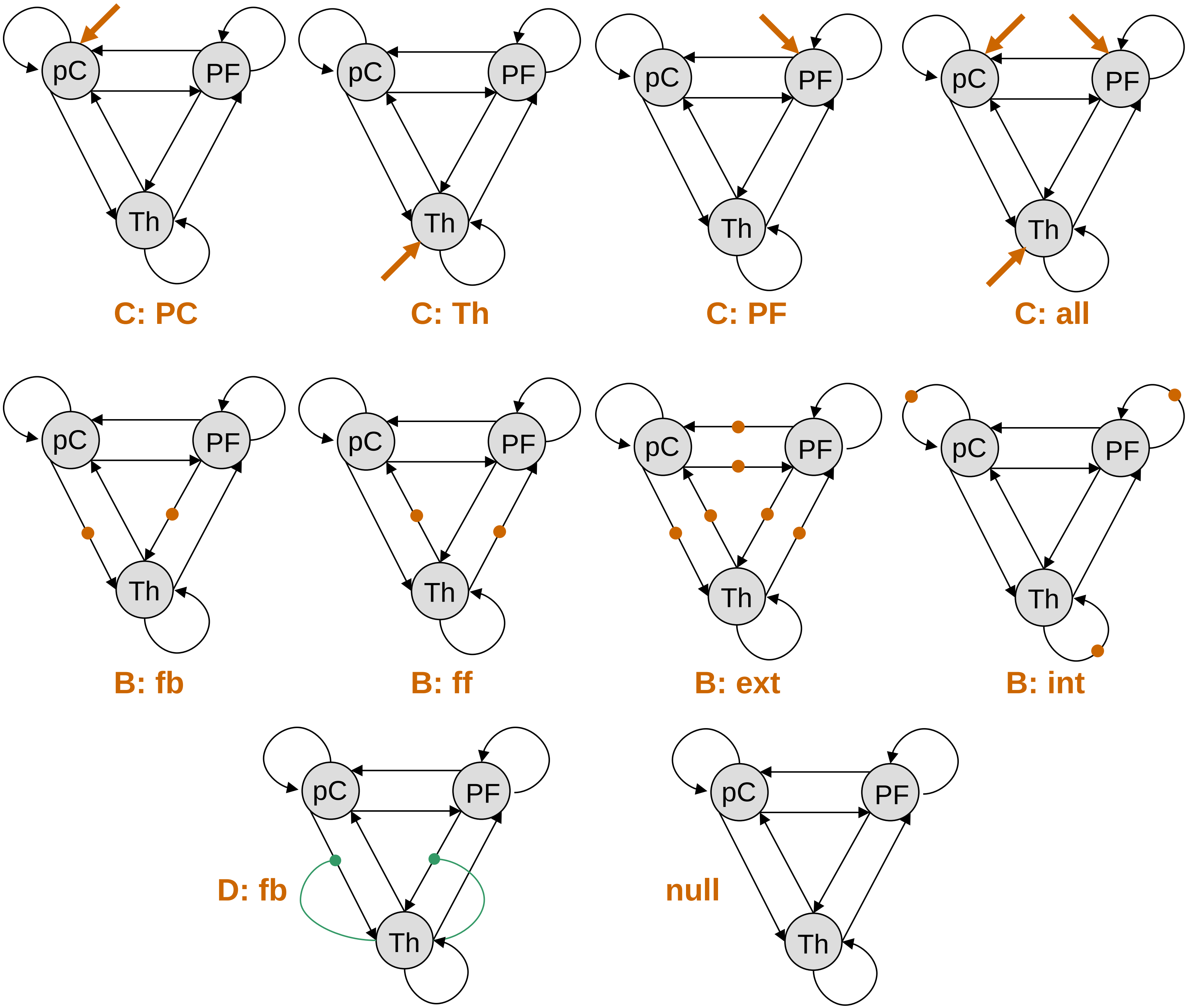
pC
PF
Th
C: PC
C: Th
C: PF
C: all
B: fb
B: ff
B: ext
B: int
D: fb
null

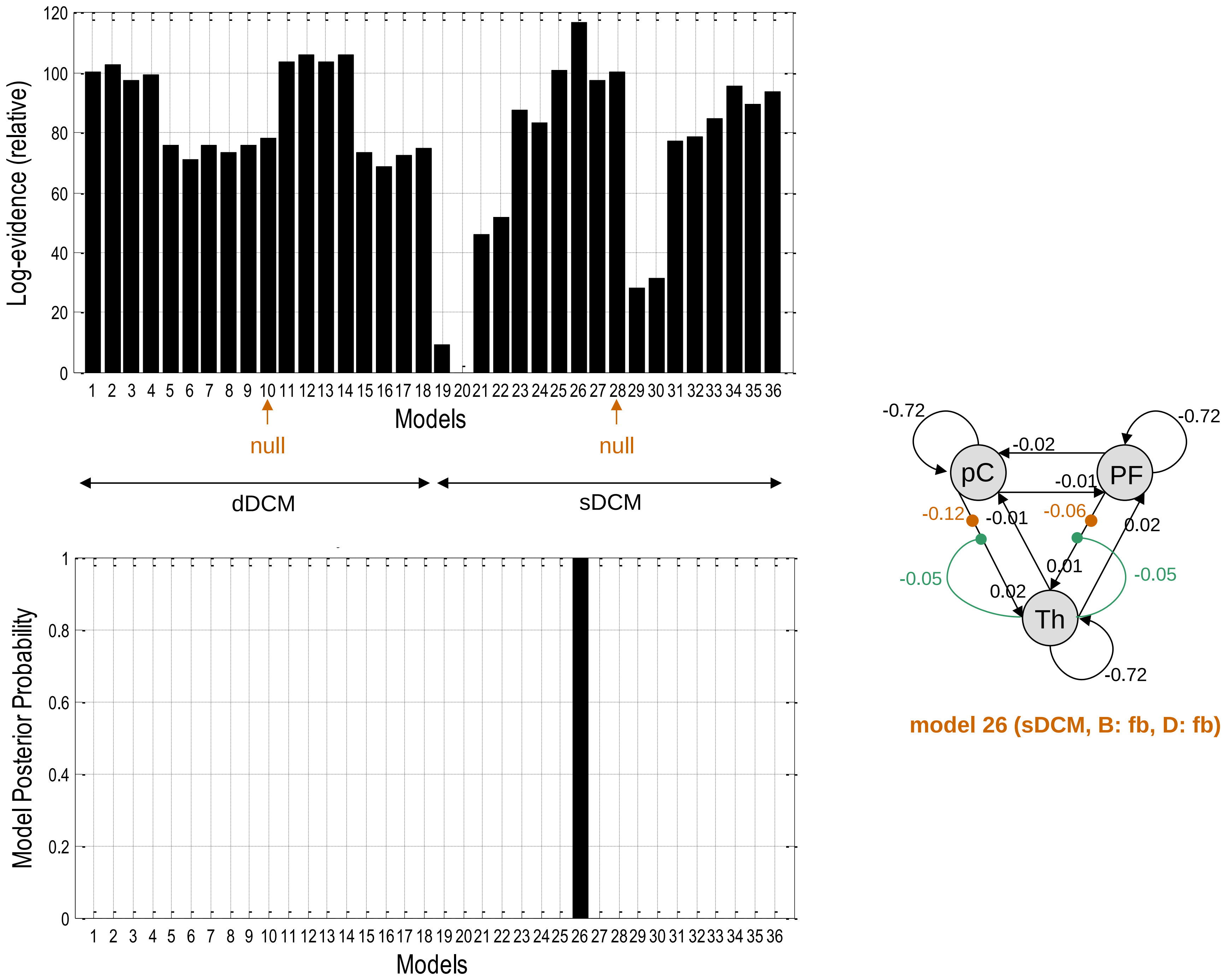
Log-evidence (relative)
Models
null
null
dDCM
sDCM
Model Posterior Probability
Models
-0.72
-0.72
-0.72
pC
PF
Th
-0.02
-0.01
-0.12
-0.01
-0.06
0.02
-0.05
0.01
-0.05
0.02
model 26 (sDCM, B: fb, D: fb)

Overview

1. Embedding computational models in DCM
2. Integrating tractography with DCM
3. Stochastic DCM
4. Optimizing experimental design
5. Searching through large model spaces
6. Some diagnostic on inversion results
7. Experimental validation and perspectives

Optimizing experimental design

new competing hypotheses
about a neural system

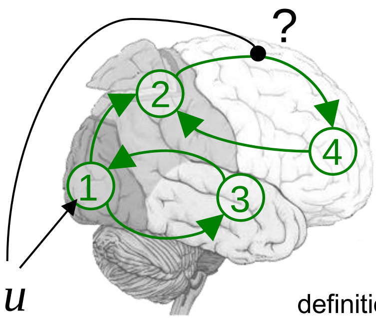

definition of a set of candidate
DCMs as neural system models

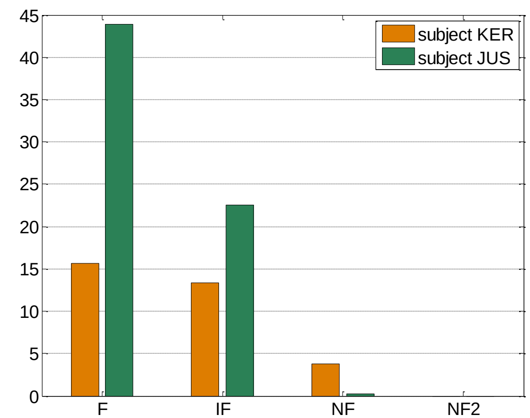

time series analysis:
Bayesian model comparison
of candidate DCMs

design an experimental study
to discriminate among
candidate DCMs

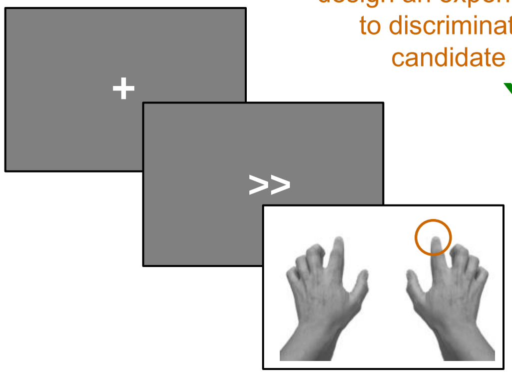

data acquisition
and selection of
activated ROIs

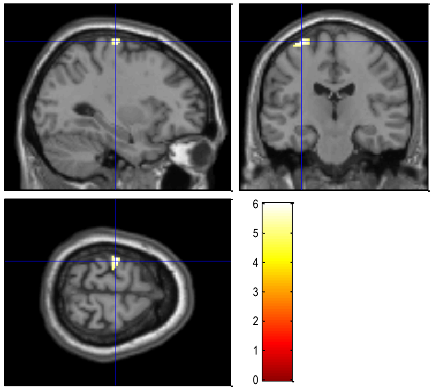

Daunizeau et al., 2011

Bayesian model selection risk

discriminability of prior predictive densities

$$b_{LC}(u) = 1 - \frac{1}{2}\log\left(\frac{\Delta g(u)^2}{4\tilde{Q}(u)} + 1\right) \qquad \text{if} \quad \tilde{Q}_1(u) \approx \tilde{Q}_2(u) \equiv \tilde{Q}(u)$$

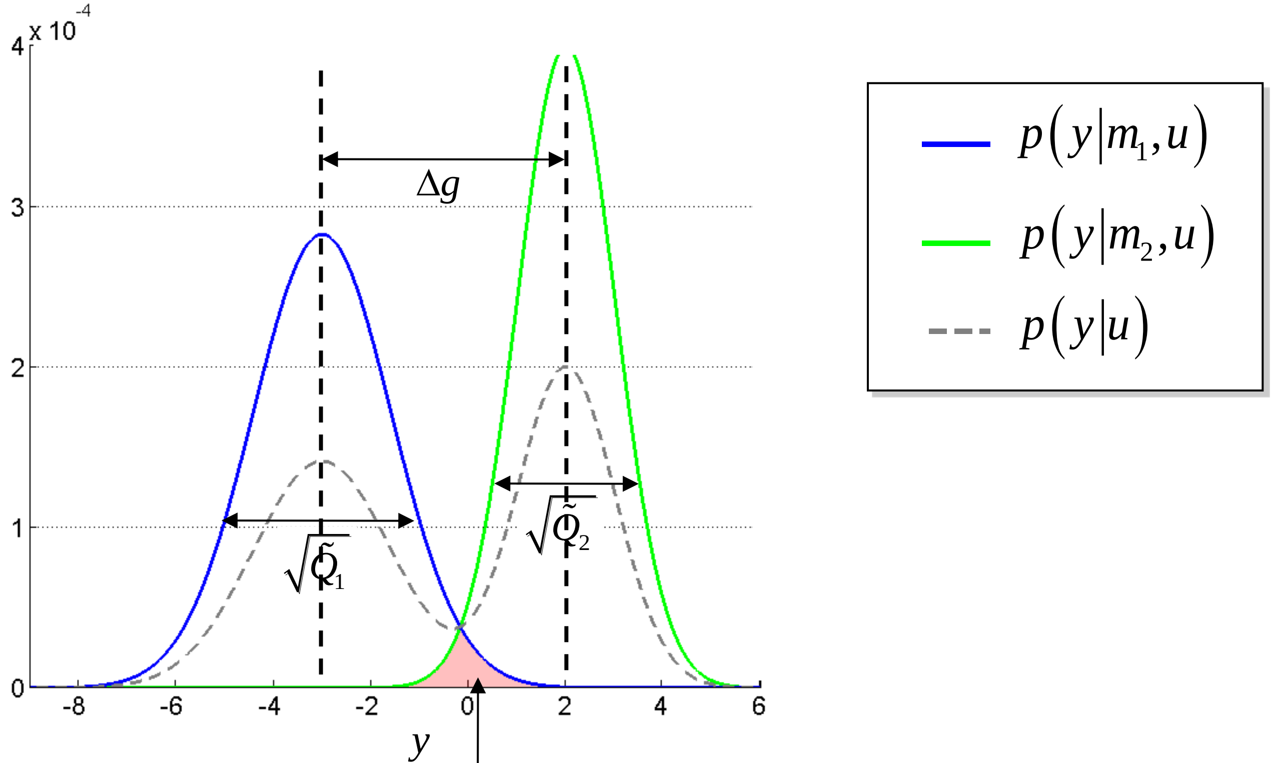

$$p(\hat{e}=1|u) = 1 - \int_Y \max_m \left[p(m)\, p(y|m,u) \right] dy$$

Daunizeau et al., 2011

design risk for DCM analysis

canonical network identification questions (I)

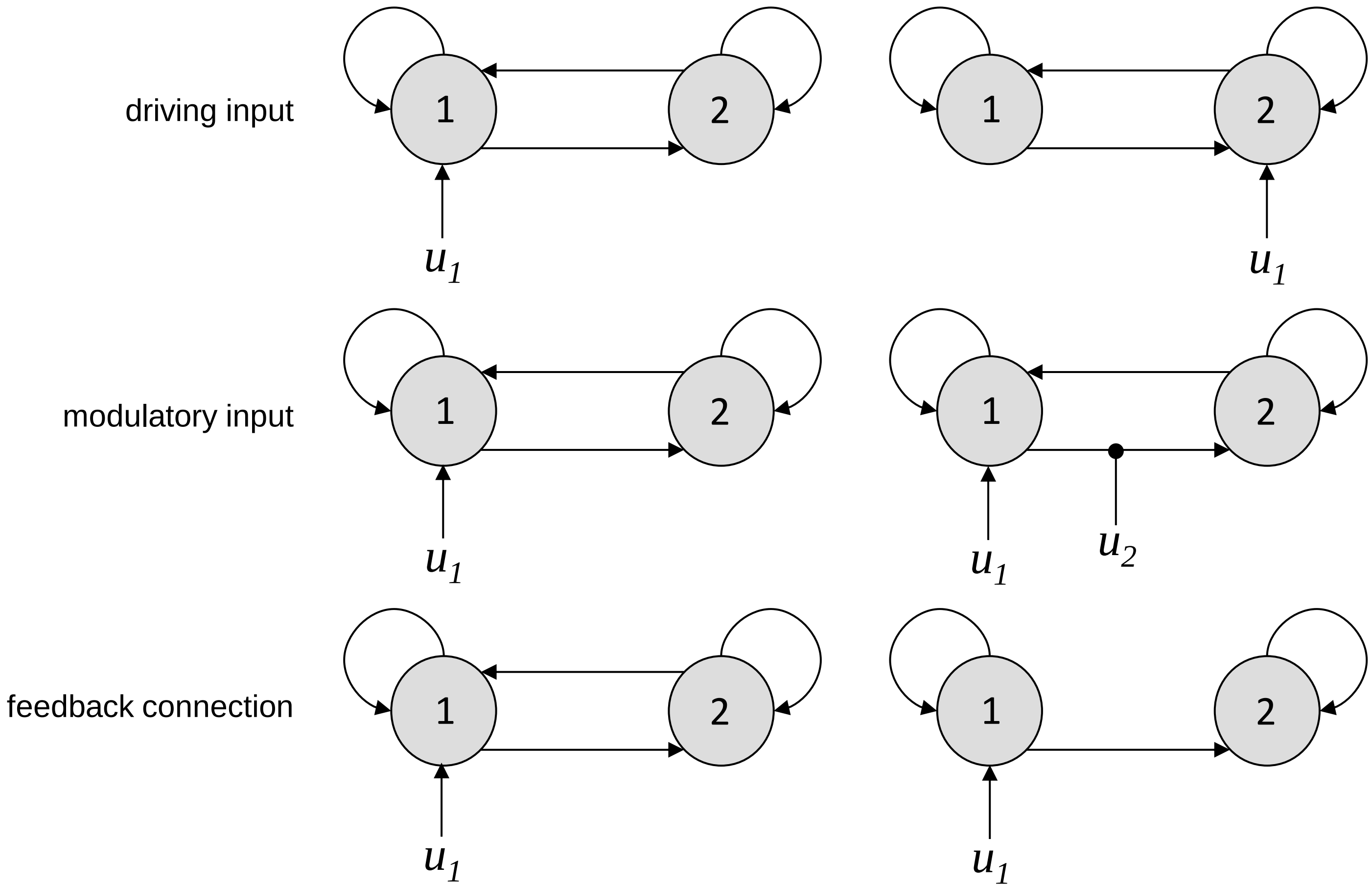

Daunizeau et al., 2011

design risk for DCM analysis

canonical network identification questions (II)

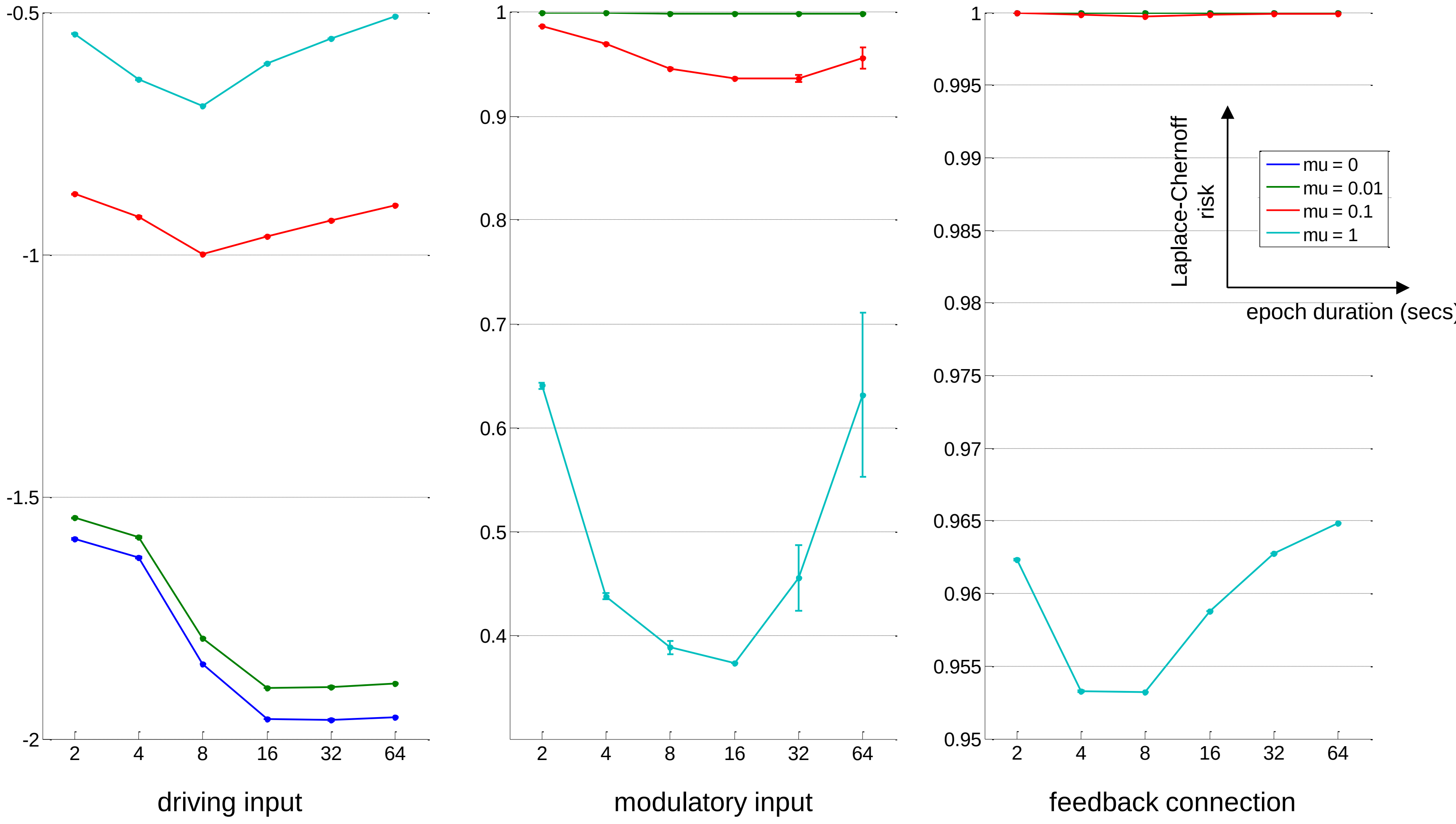

Daunizeau et al., 2011

design risk for DCM analysis

identifying psycho-physical interactions (I)

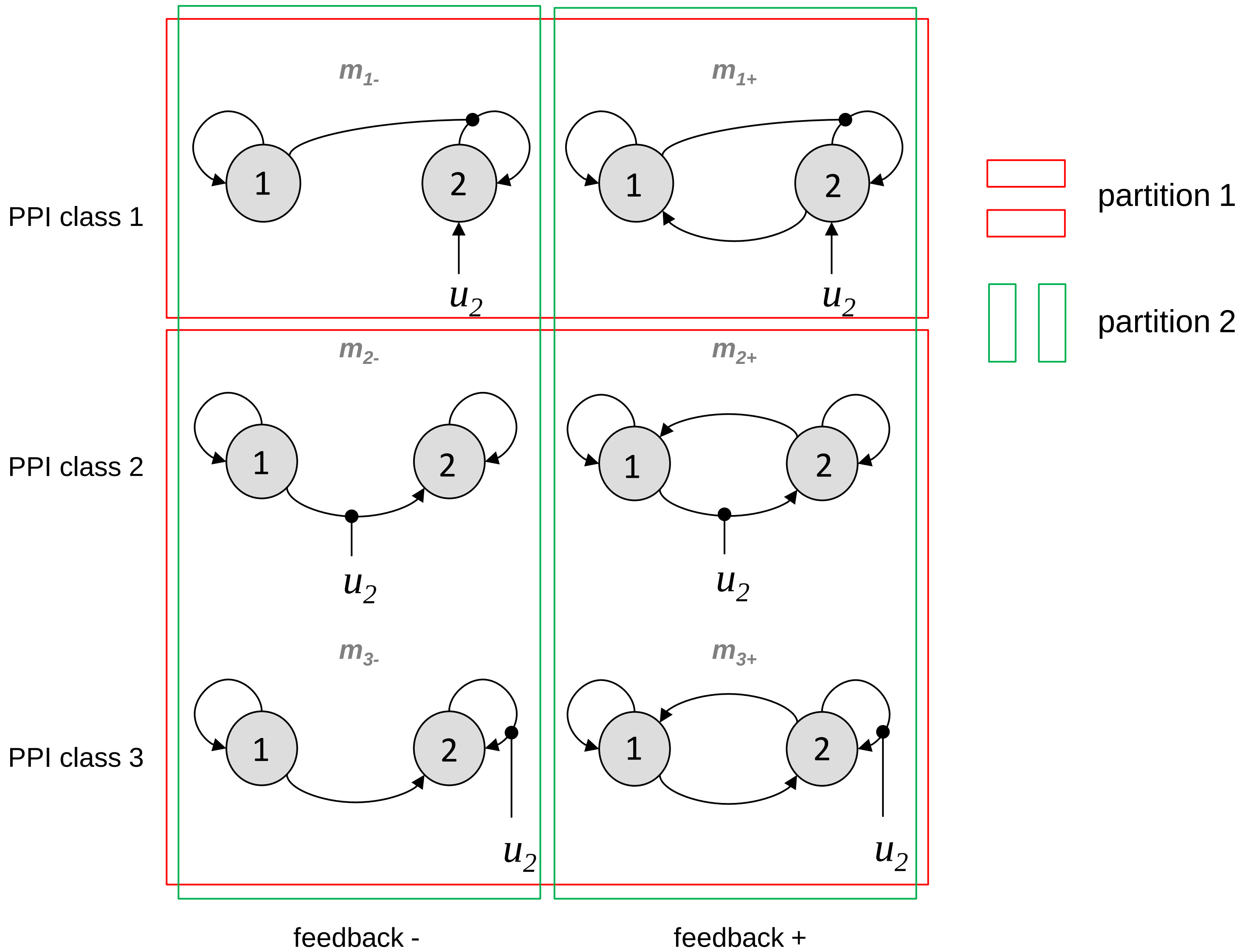

Daunizeau et al., 2011

design risk for DCM analysis

identifying psycho-physical interactions (II)

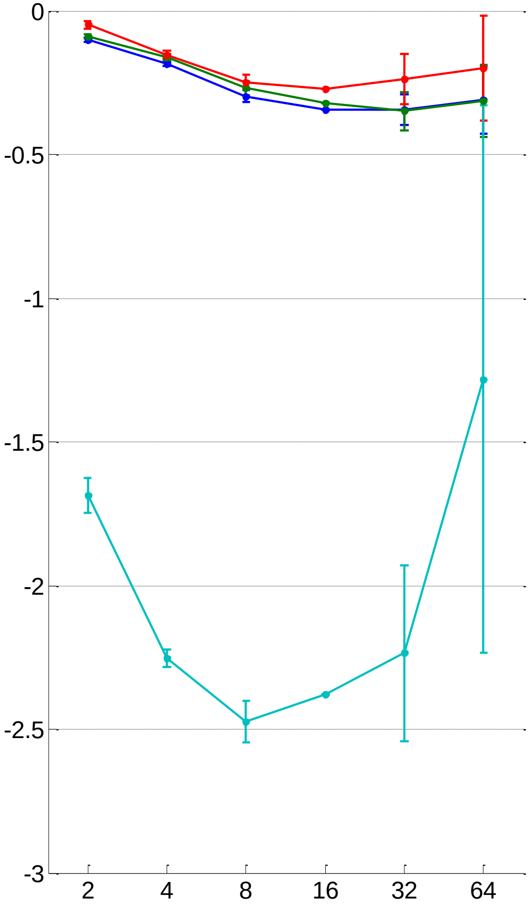

PPI: partition 1

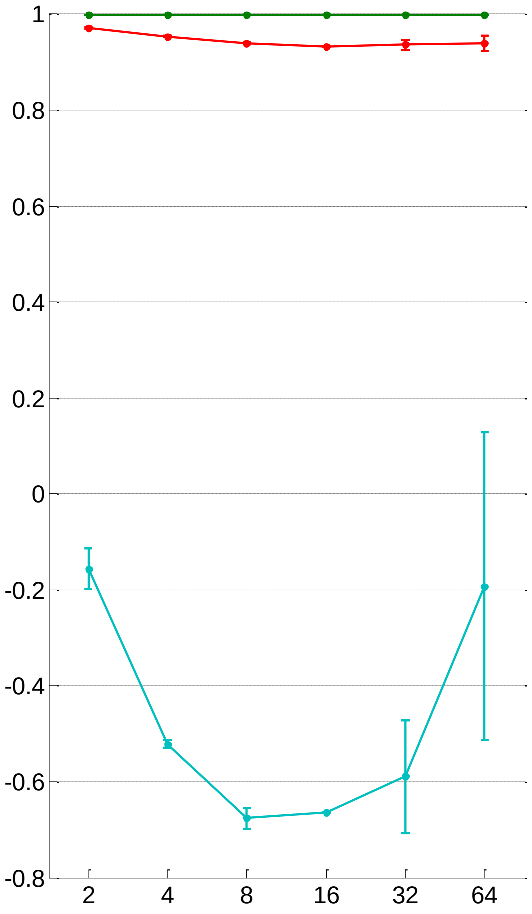

PPI: partition 2

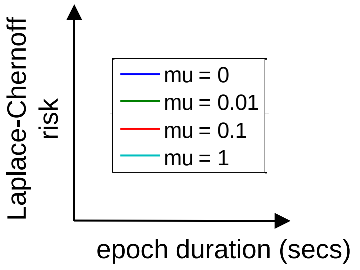

Daunizeau et al., 2011

design risk for DCM analysis

identifying psycho-physical interactions (III)

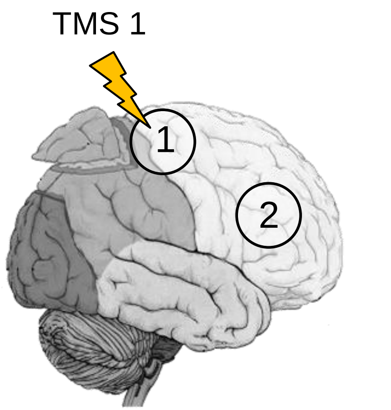

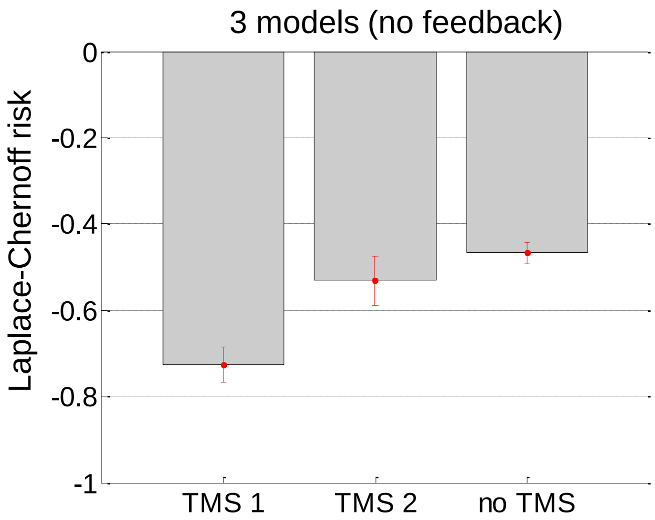

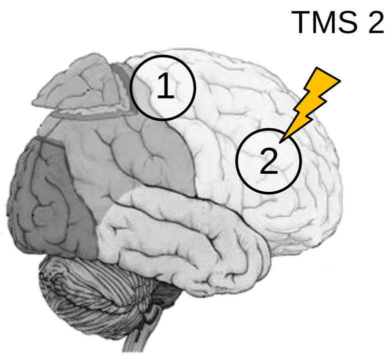

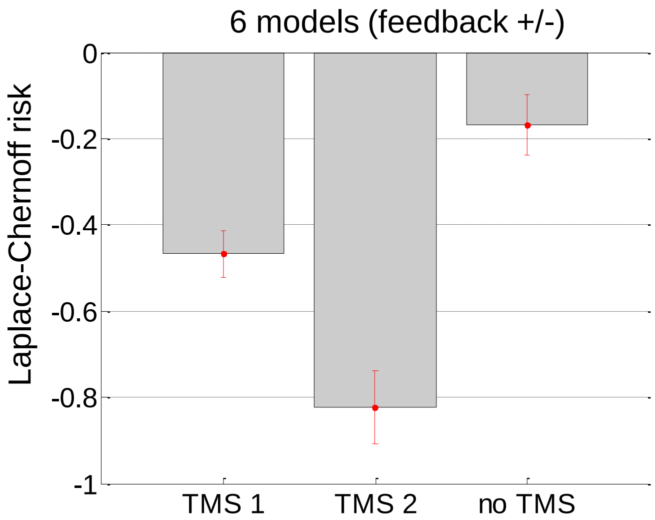

Daunizeau et al., 2011

Overview

1. Embedding computational models in DCM
2. Integrating tractography with DCM
3. Stochastic DCM
4. Optimizing experimental design
5. Searching through large model spaces
6. Some diagnostic on inversion results
7. Experimental validation and perspectives

Searching through large model spaces

the Savage-Dickey ratio

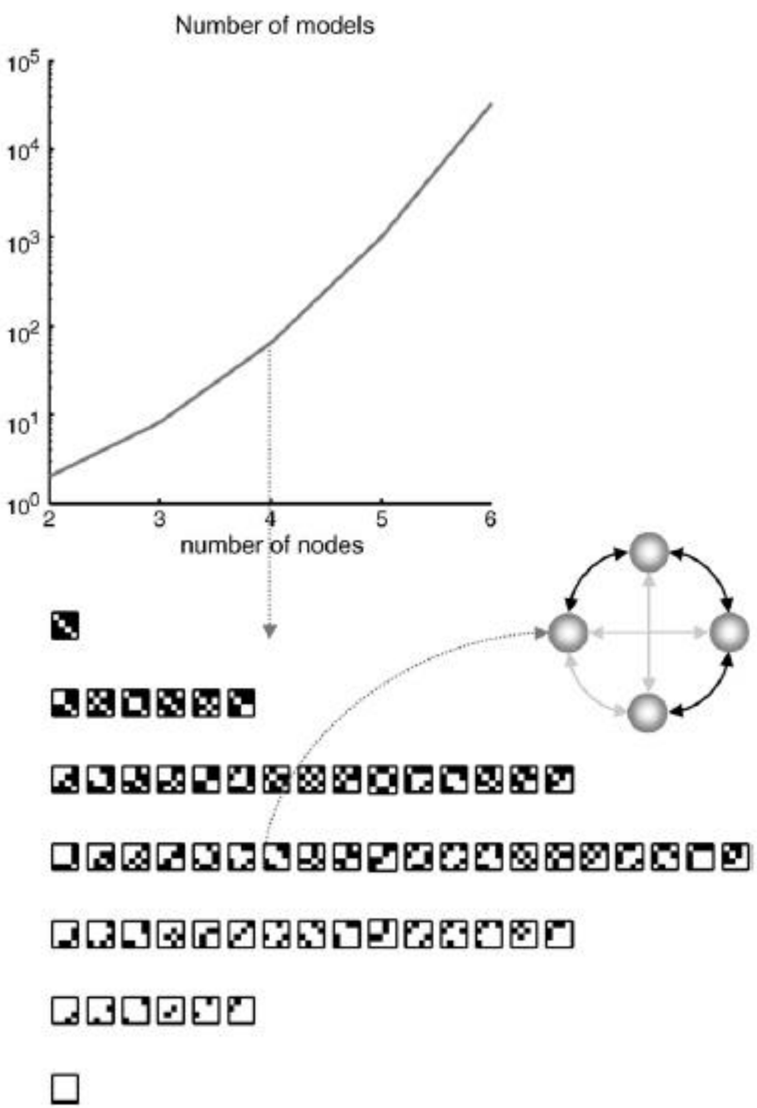

→ reduced model: $m_i : \begin{cases} \theta_i = 0 \\ \theta_{\setminus i} \neq 0 \end{cases}$

$$\frac{p(y|m_i)}{p(y|m_{full})} = \frac{p(\theta_i = 0|y, m_{full})}{p(\theta_i = 0|m_{full})}$$

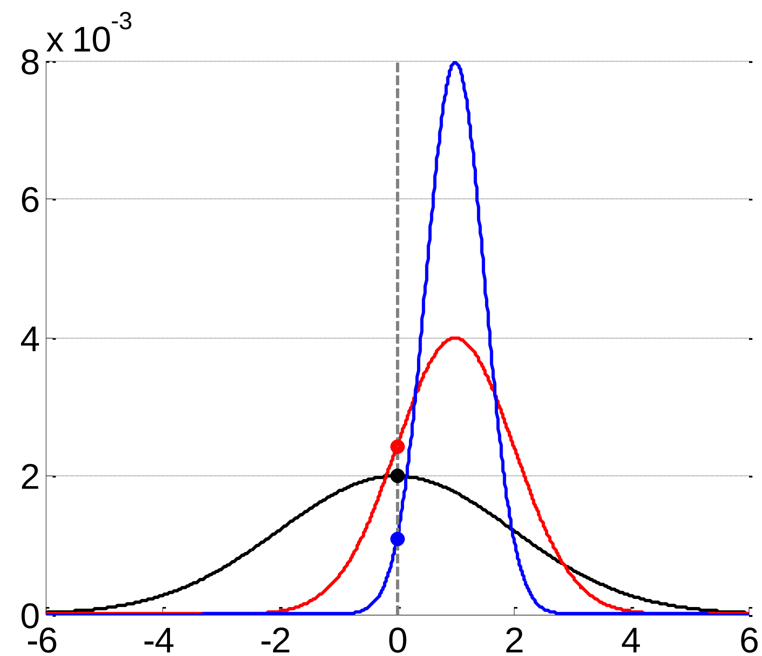

Friston et al., 2011

Searching through large model spaces

network discovery

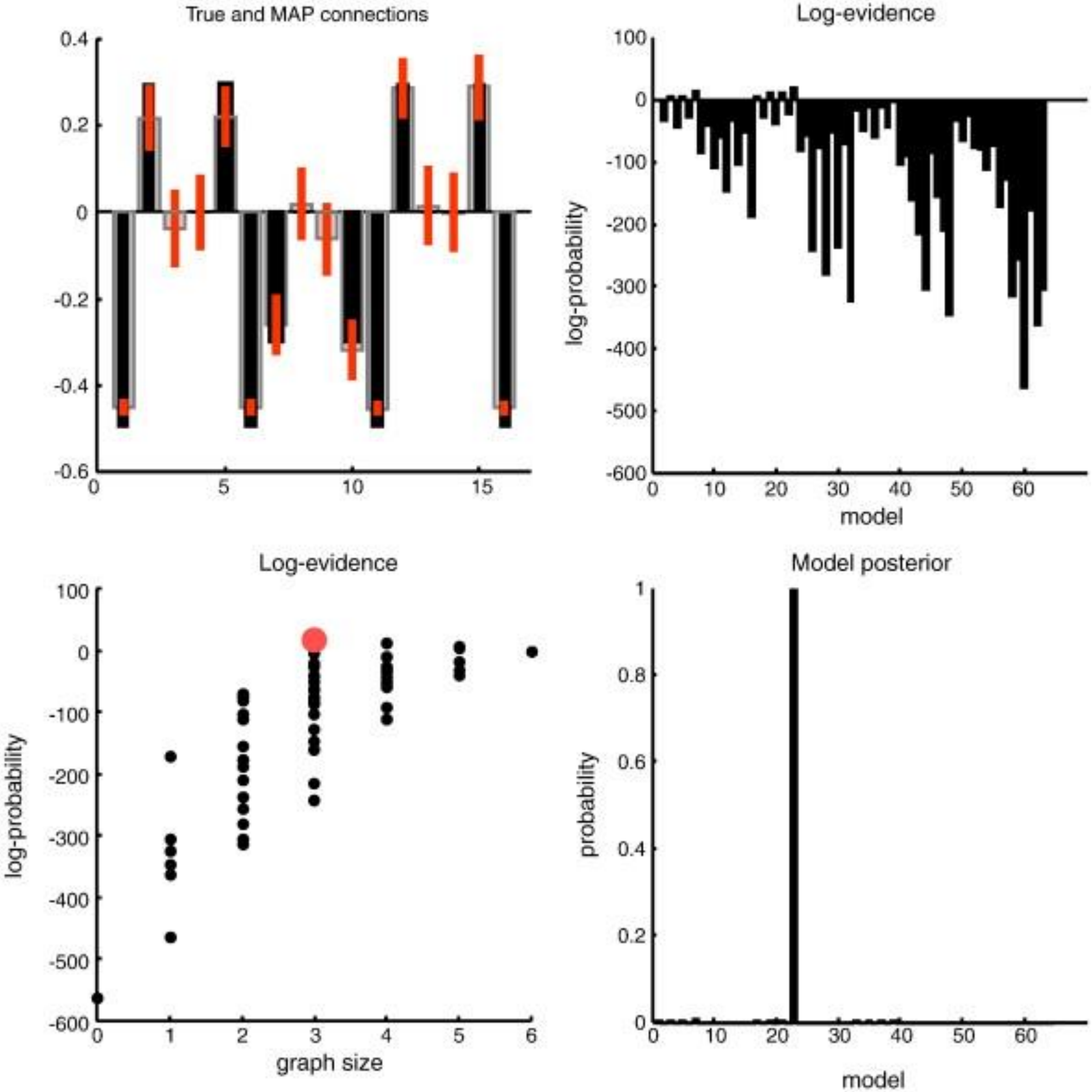

Friston et al., 2011

Searching through large model spaces

how does Savage-Dickey ratio compares to model inversion?

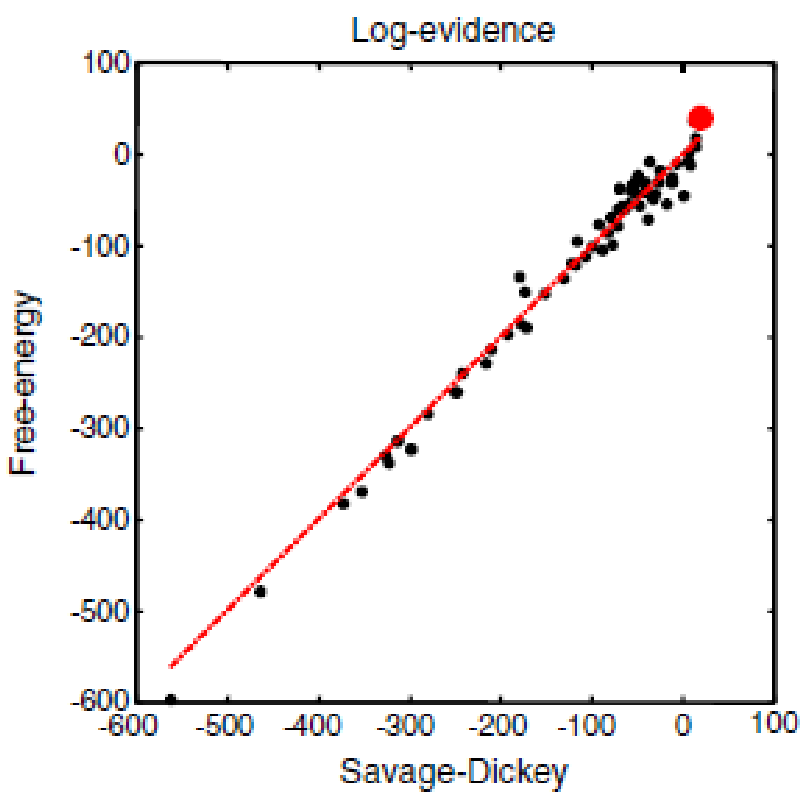

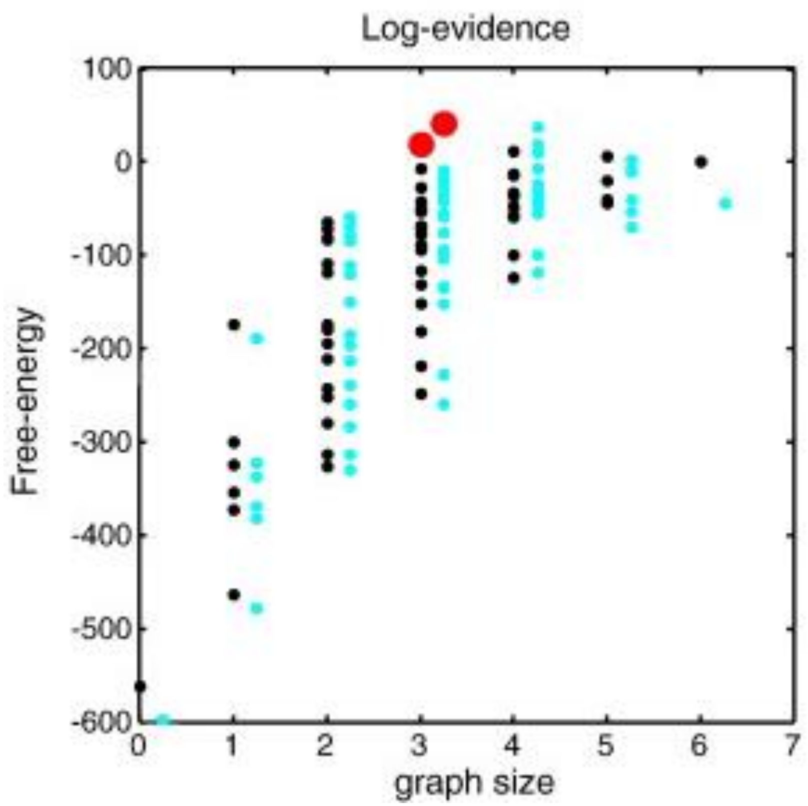

Friston et al., 2011

Overview

1. Embedding computational models in DCM
2. Integrating tractography with DCM
3. Stochastic DCM
4. Optimizing experimental design
5. Searching through large model spaces
6. Some diagnostic on inversion results
7. Experimental validation and perspectives

Diagnosing Bayesian inversion

underfitting: residuals structure

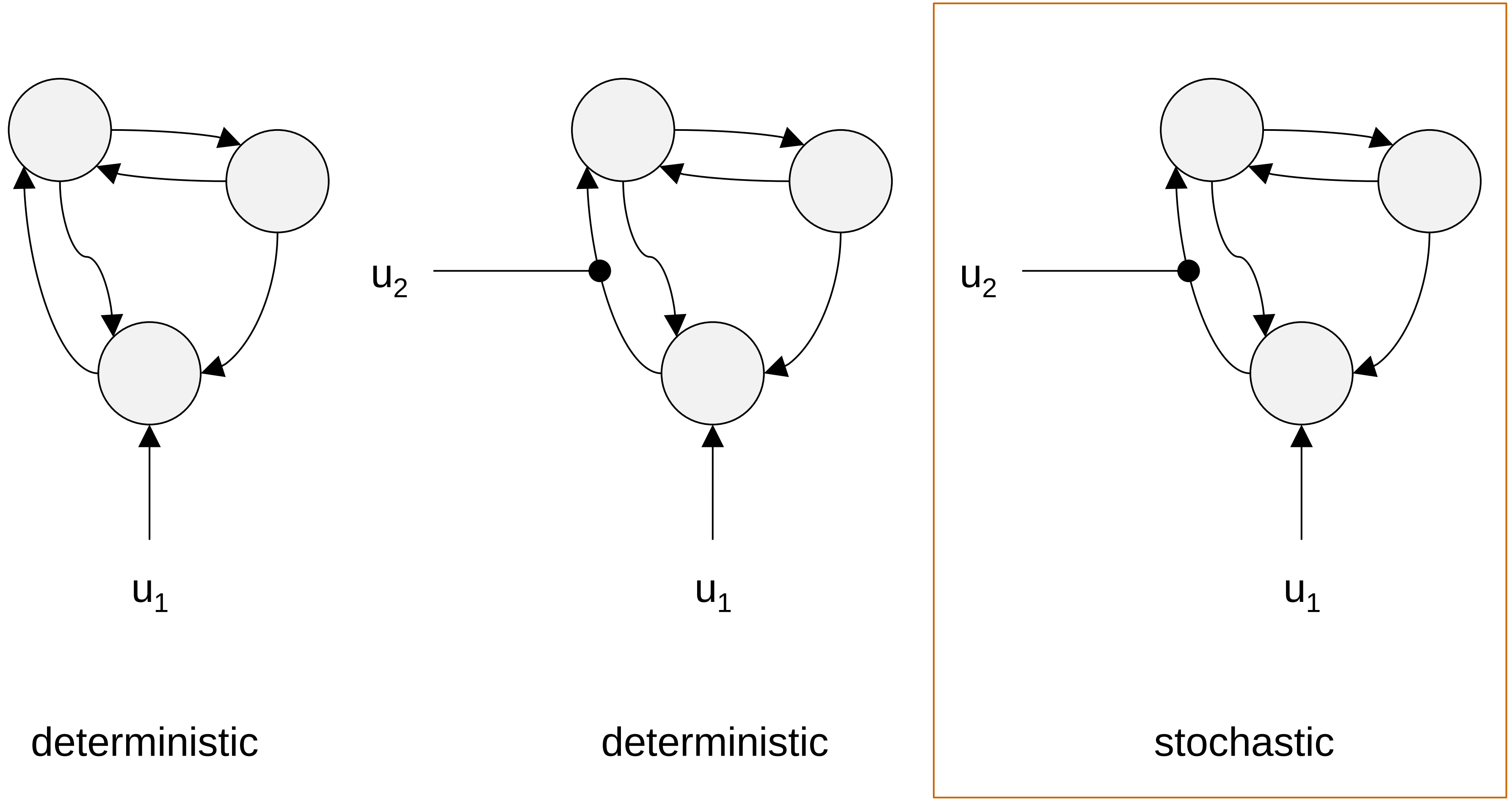

Diagnosing Bayesian inversion

underfitting: residuals structure

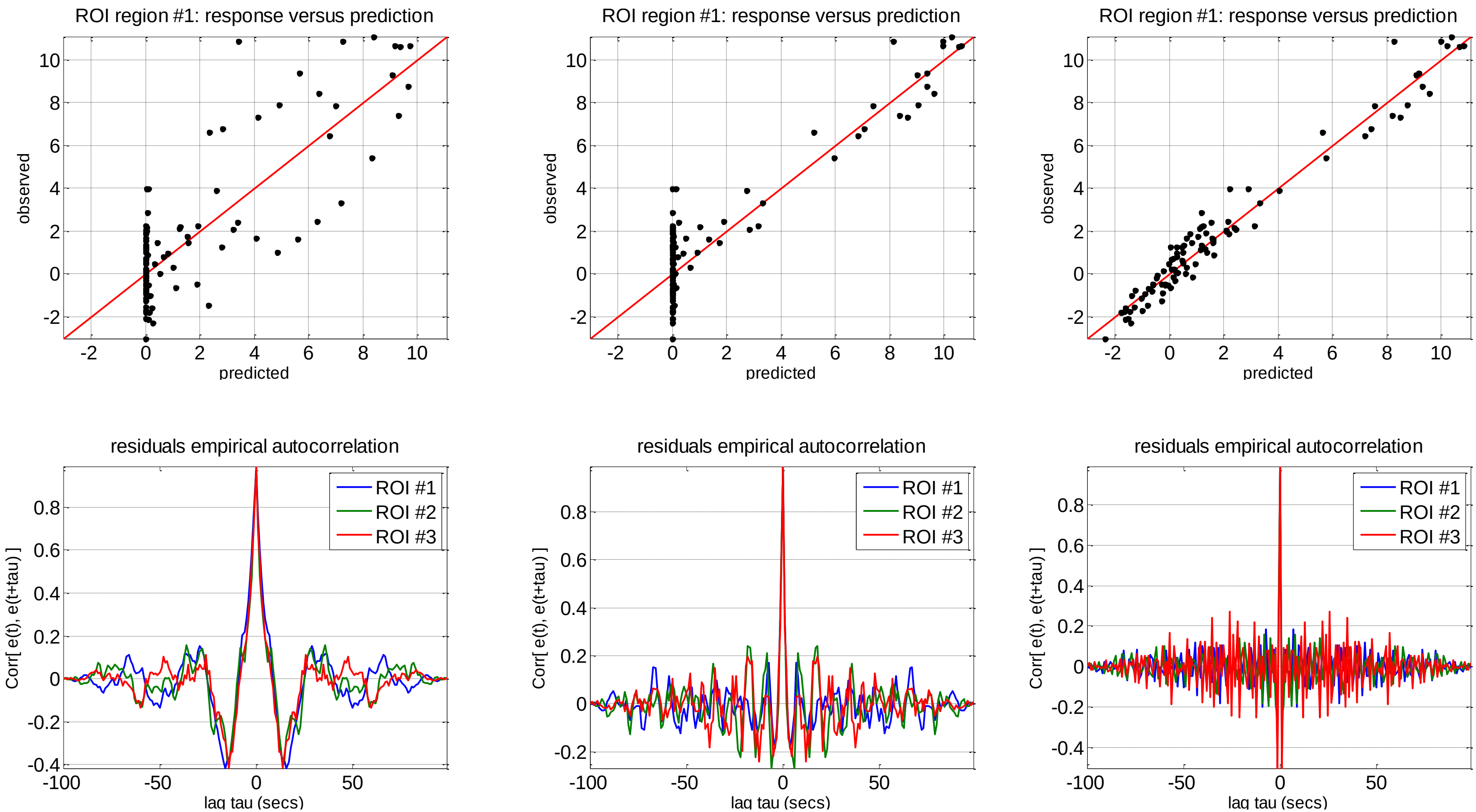

F=-824.2 F=-694.9 F=-658.7

Diagnosing Bayesian inversion

identifiability: parameters' covariance matrix

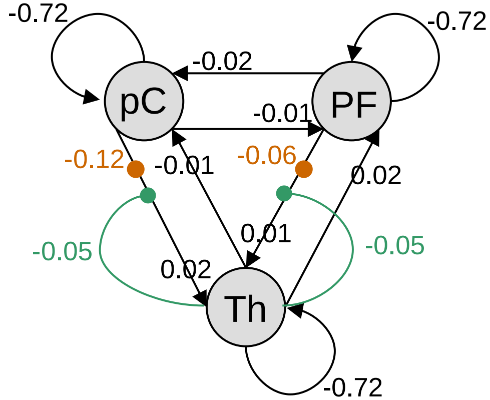

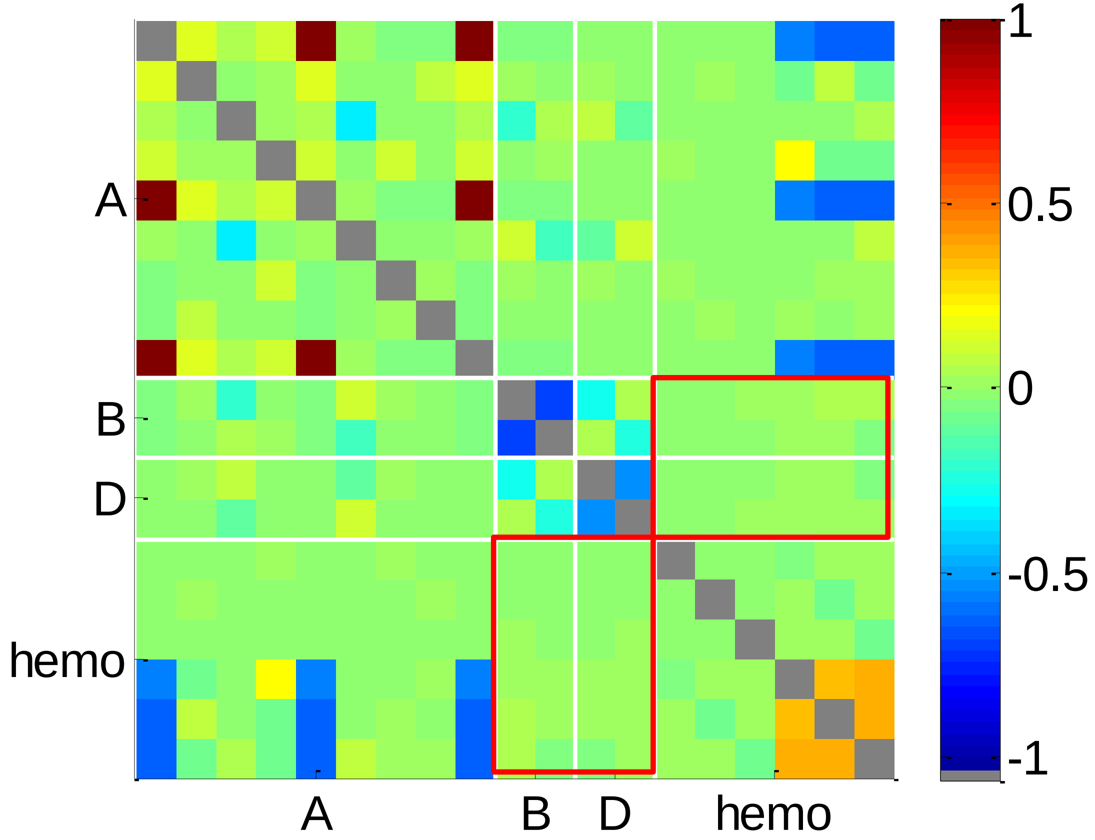

Overview

1. Embedding computational models in DCM
2. Integrating tractography with DCM
3. Stochastic DCM
4. Optimizing experimental design
5. Searching through large model spaces
6. Some diagnostic on inversion results
7. Experimental validation and perspectives

Experimental validation (I)

EEG setup of the recording session

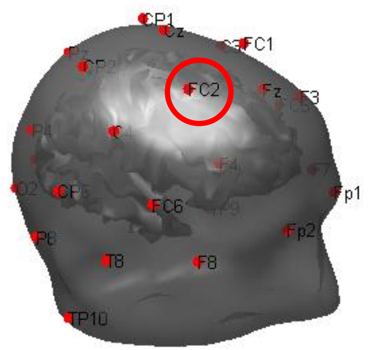

best channel fit: EEG frequency modulation

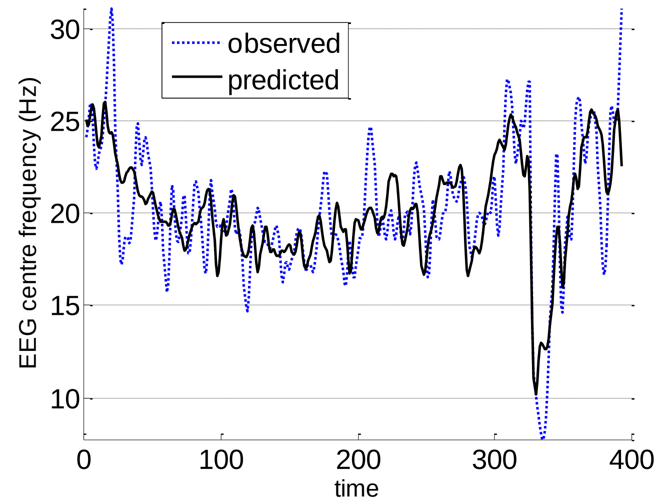

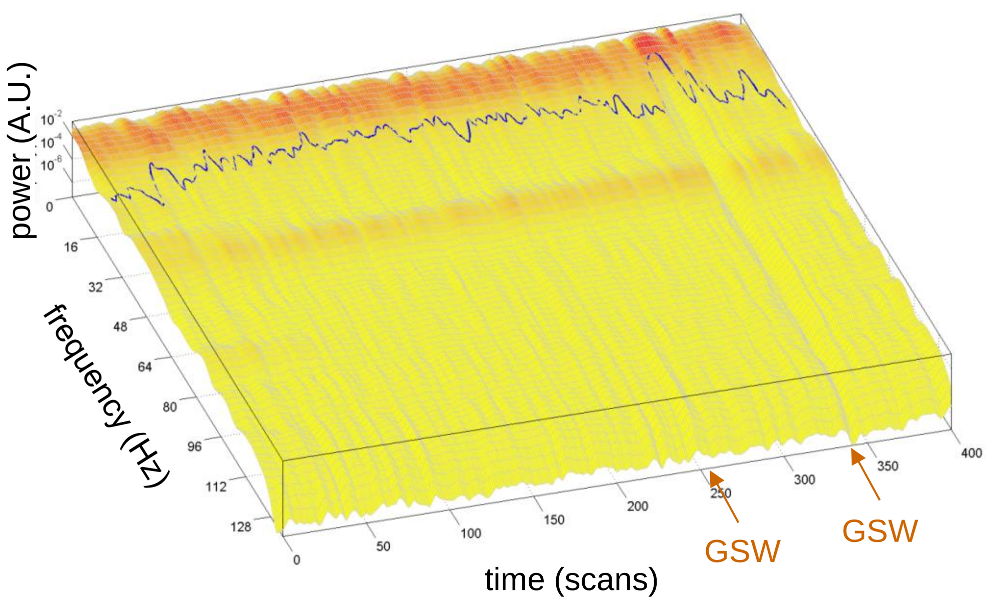

P(x>5.000e-001) = 9.913e-001

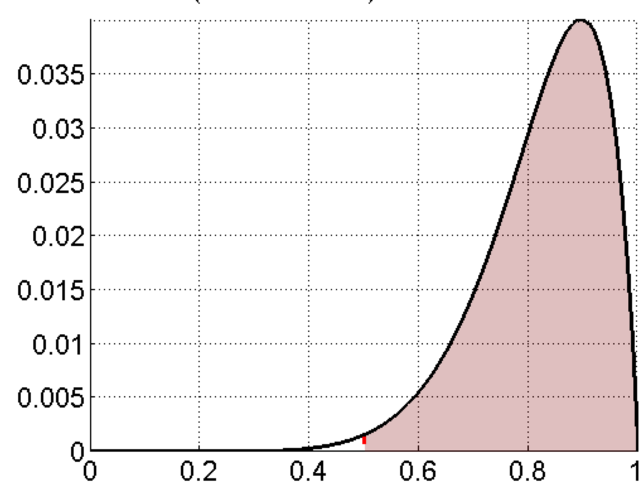

$$P\left(f_{H_1} > 0.5 \middle| \bar{\omega}\right) \approx 0.99$$

Experimental validation (II)

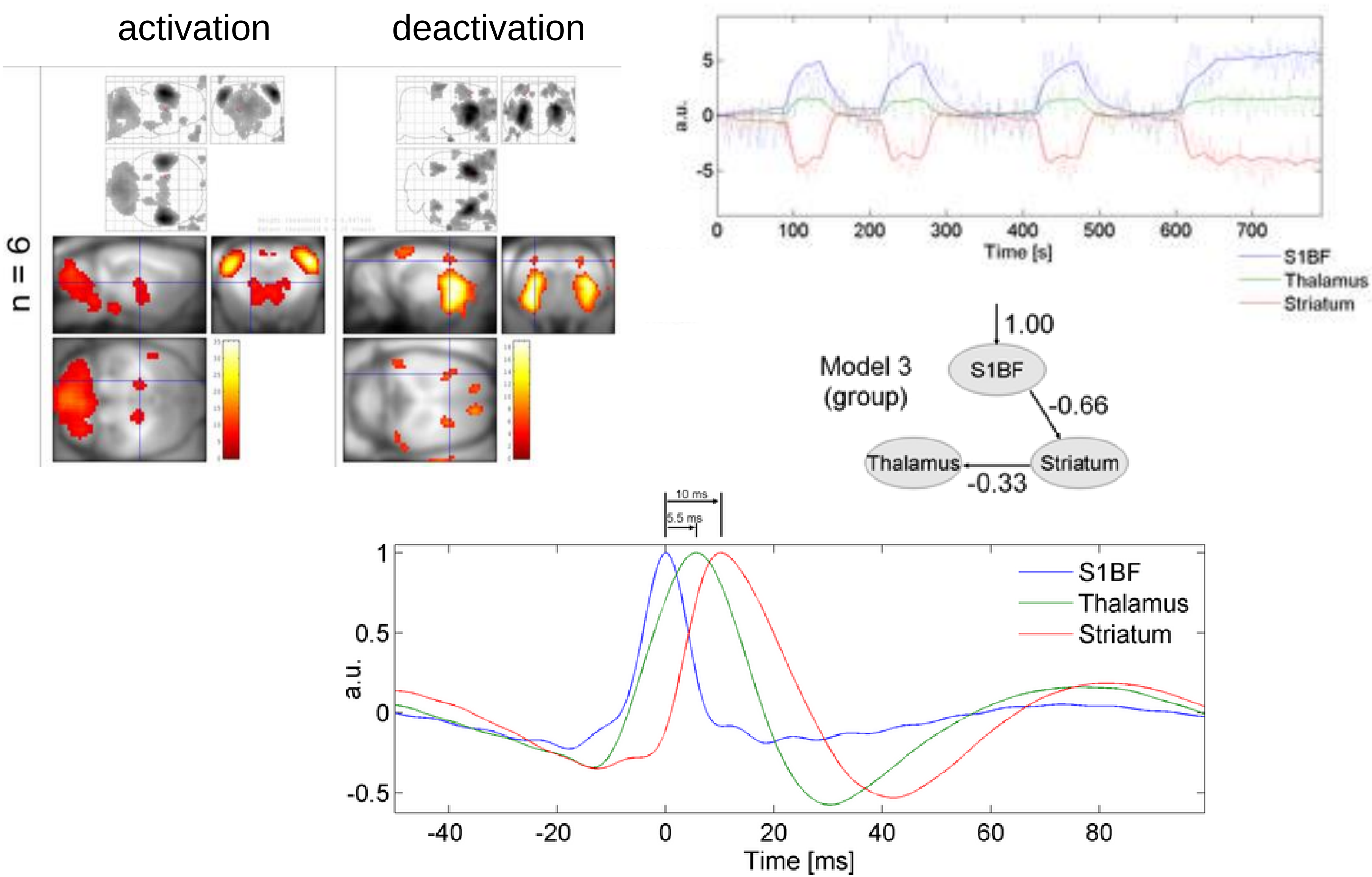

David et al., 2008

Perspectives

augmenting DCM with a behavioural output: principle

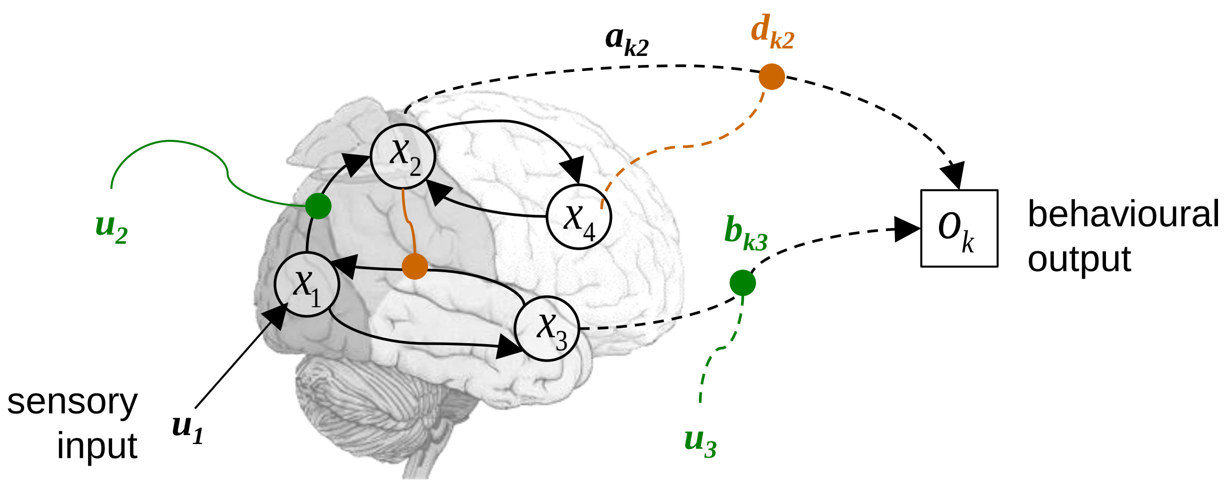

✓ modelling the brain input-output transform (through the network)

✓ decomposing the relative contribution of brain regions and their interactions to the behavioural response

Perspectives

augmenting DCM with a behavioural output: example (I)

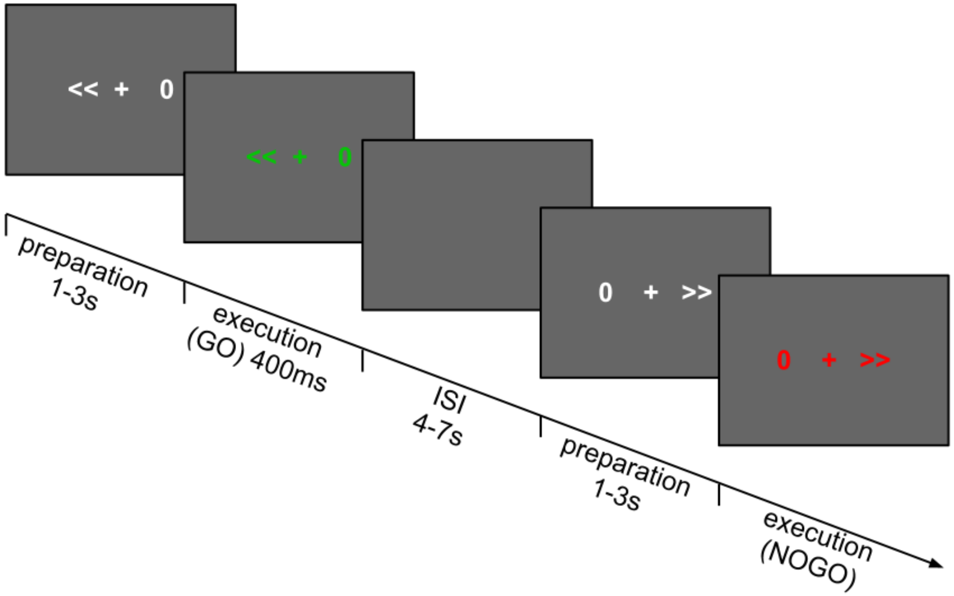

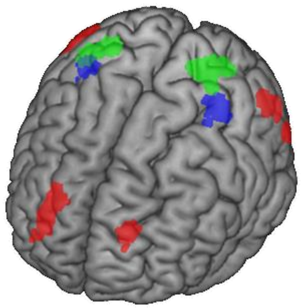

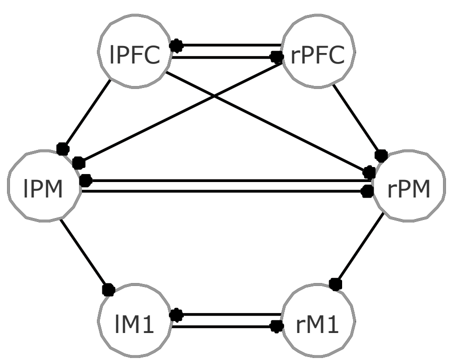

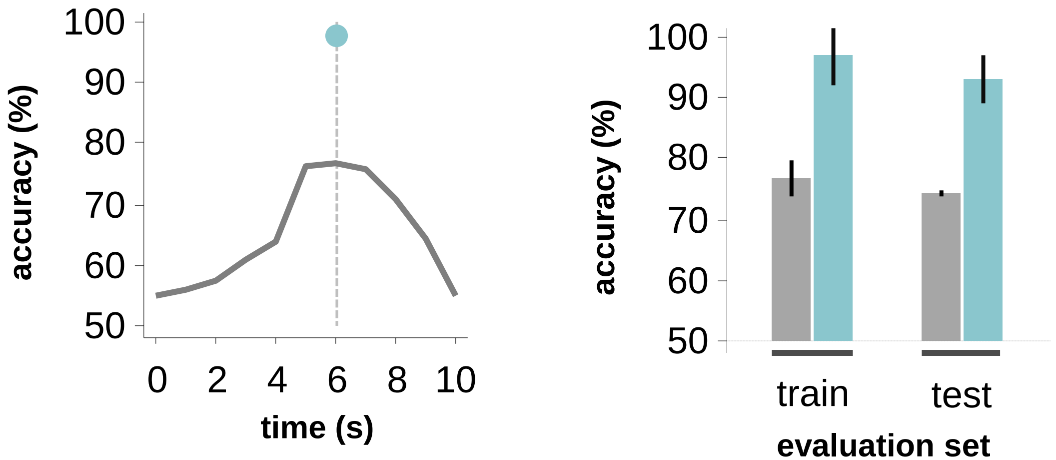

Perspectives

augmenting DCM with a behavioural output: example (II)

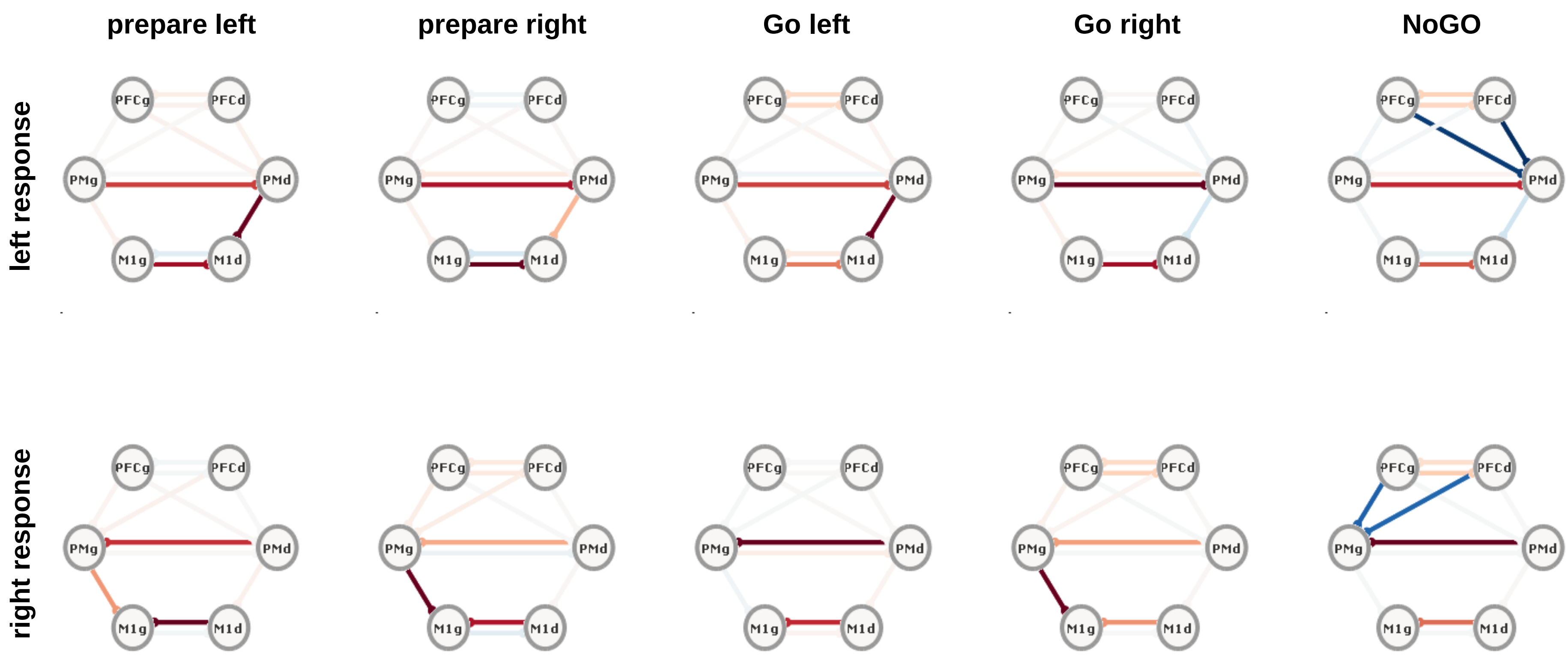

References

Daunizeau et al., 2012: Stochastic Dynamic Causal Modelling of fMRI data: should we care about neural noise? Neuroimage,62: 464-481.

Daunizeau et al., 2011: Optimizing experimental design for comparing models of brain function. PLoS Comp. Biol., 7(11): e1002280

Friston et al. ,2011: Network discovery with DCM. Neuroimage, 56: 1202-1221.

Den Ouden et al., 2010: Striatal prediction error modulates cortical coupling. J. Neurosci, 30: 3210-3219.

Stephan et al., 2009: Tractography-based priors for dynamic causal models. Neuroimage 47: 1628-1638.

Kaden et al., 2007: Bayesian analysis of anatomical connectivity using diffusion MRI. Neuroimage 27: 474-488.

Parker et al., 2005: Probabilistic anatomical connectivity derived from the microscopic persistent angular structure of cerebral tissue. Trans. R. Soc. London, 360: 893-902.

Many thanks to:

Kerstin Preuschoff (EPFL, Lausanne, Switzerland)
Karl J. Friston (FIL, London, UK)
Klaas E. Stephan (UZH, Zurich, Switzerland)
Lionel Rigoux (ICM, Paris, France)